Research Paper

Landscape of the oncogenic role of fatty acid synthase in human tumors

Xulei Huo[1,2], Lairong Song[1,2], Da Li[1,2], Ke Wang[1,2], Yali Wang[3,4], Feng Chen[3,4], Liwei Zhang[1,2], Liang Wang[1,2], Junting Zhang[1,2], Zhen Wu[1,2]

[1]Department of Neurosurgery, Beijing Tiantan Hospital, Capital Medical University, Beijing, China
[2]China National Clinical Research Center for Neurological Diseases, Beijing, China
[3]Beijing Key Laboratory of Brain Tumor, Beijing, China
[4]Department of Neuro-Oncology, Cancer Center, Beijing Tiantan Hospital, Capital Medical University, Beijing, China

Correspondence to: Liang Wang, Zhen Wu; **email:** wangliang@bjtth.org, wuzhen@bjtth.org
Keywords: fatty acid synthase, tumor, expression, prognosis, phosphorylation, methylation, tumor-infiltrating immune cell
Received: September 7, 2021 **Accepted:** November 24, 2021 **Published:** December 8, 2021

ABSTRACT

Background: Identifying a unique and common regulatory pathway that drives tumorigenesis in cancers is crucial to foster the development of effective treatments. However, a systematic analysis of fatty acid synthase across pan-cancers has not been carried out.
Methods: We investigated the oncogenic roles of fatty acid synthase in 33 cancers based on the cancer genome atlas and gene expression omnibus.
Results: Fatty acid synthase is profoundly expressed in most cancers and is an important factor in predicting the outcome of cancer patients. Further, the level of S207 phosphorylation was found to be improved in several neoplasms (e.g., colon cancer). Fatty acid synthase expression is related to tumor-infiltrating immune cells in tumors (e.g., CD8+ T-cell infiltration level in cervical squamous cell carcinoma). Moreover, hormone receptor binding- and fatty acid metabolic process-associated pathways are involved in the functional mechanisms of fatty acid synthase.
Conclusions: This study provides a complete understanding of the oncogenic role of fatty acid synthase in human tumors.

INTRODUCTION

The identification and portrayal of novel oncogenic genes are critical for gaining a more comprehensive understanding of the complicated course of tumorigenesis owing to the intricacy of this process. The Cancer Genome Atlas (TCGA) project and gene expression omnibus (GEO) dataset contain useful genomic information sets of various tumors [1–3] and can be employed to identify the potential oncogenic role of fatty acid synthase (FASN).

Endogenous fatty acid synthesis is catalyzed by FASN, a human lipogenic enzyme capable of *de novo* synthesis of fatty acids [4, 5]. The functional roles of FASN have been assessed in different species from the perspectives of physiology and pathology [6–9]. The human FASN protein is composed of six catalytic units. Starting from the N-terminus, these units include β-ketoacyl synthase (KS), acetyl/malonyl transacylase (AT/MT), β-hydroxyacyl dehydratase (DH), enoyl reductase (ER), β-ketoacyl reductase (KR), acyl carrier protein (ACP), and thioesterase (TE). The relationship between FASN and tumorigenesis of bladder cancer [10], meningioma [11], and breast cancer [12, 13] has been reported. In this study, we summarized laboratory-based results from cell or animal experiments with regarding to the relationship between FASN and various malignancies

(Figure 1). Of note, no correlation was found between FASN and pan-cancer.

For our investigation, we utilized TCGA project and GEO datasets. Additionally, several features (e.g., gene expression, survival prognosis, genetic alteration, DNA methylation, protein phosphorylation, immune cells, or relevant cellular pathways) were gathered to evaluate the regulatory mechanism of FASN in the tumorigenesis of cancers.

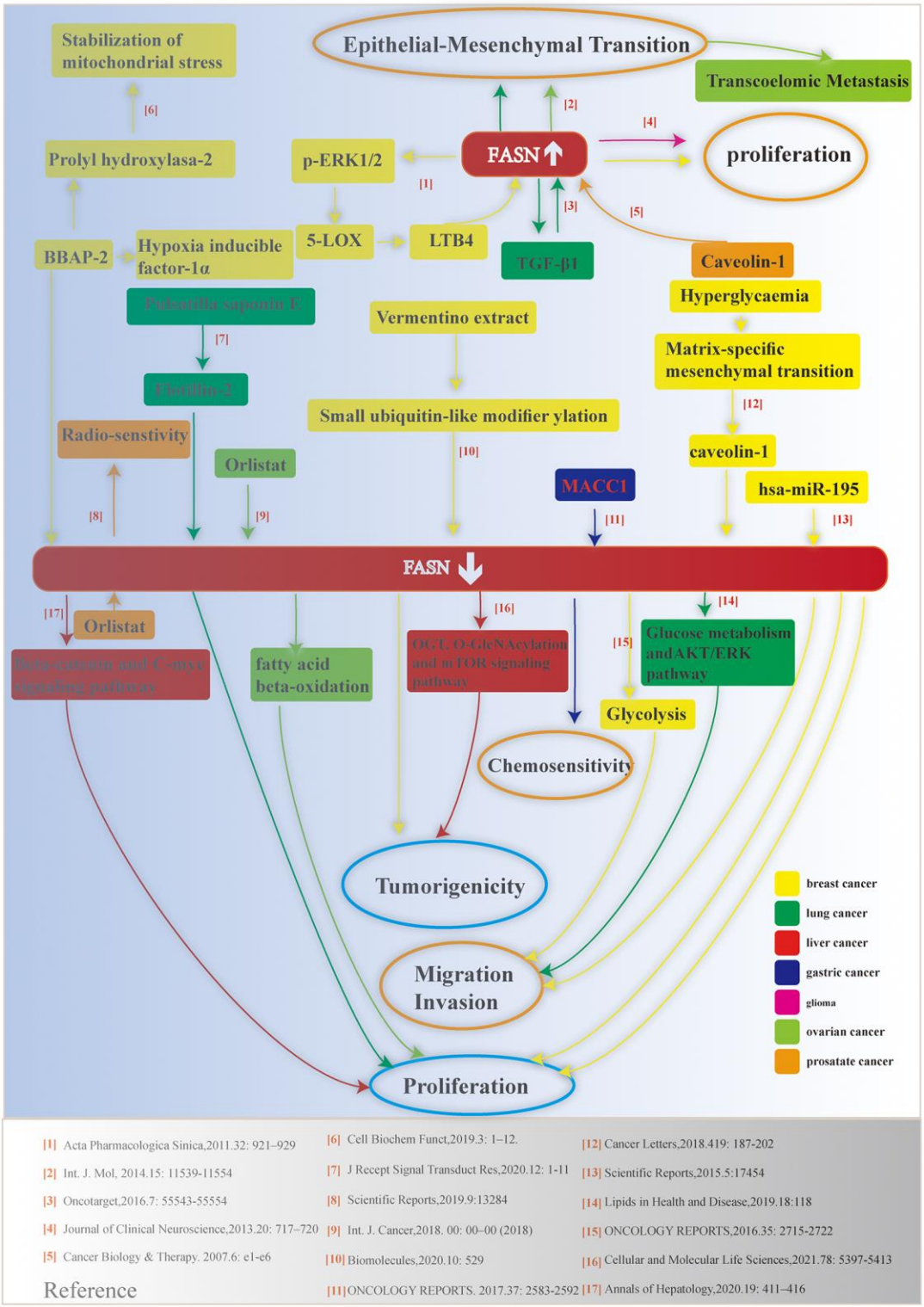

Figure 1. Schematic depicting the relationship between FASN and various cancers. Relevant references are indicated.

MATERIALS AND METHODS

Gene mapping and protein structure analysis

Based on the UCSC genome browser on human Dec. 2013 (GRCh38/hg38) assembly [14], information related to the genome location of the *FASN* gene was obtained. Further, the "HomoloGene" function of the NCBI was used to conduct conserved functional domain analysis of the FASN protein in different species. The phylogenetic status across diverse types of species were evaluated with the "COBALT" function of NCBI.

Gene expression analysis of TIMER2

We obtained the difference in FASN expression using the "Gene_DE" module of tumor immune estimation resource, version 2 (TIMER2). In tumors without contrast tissues or enough contrast group, the Gene Expression Profiling Interactive Analysis, version 2 (GEPIA2) web server [15] was utilized from the Genotype-Tissue Expression (GTEx) (P = 0.01, log2 fold change = 1).

We evaluated violin plots of FASN in various pathological stages across tumors using the "Pathological Stage Plot" module (GEPIA2). The log2 [TPM (Transcripts per million) +1] transformed expression results with a log-scale test were employed in the plots.

The Clinical Proteomic Tumor Analysis Consortium module [16] was used to determine the expression level of the total protein or phosphoprotein (S207, S724, S725, T976, S1174, S1411, S2198, and T2204 sites) of FASN (NP_004595.4) between cancers and corresponding tissue, respectively. Six tumors were screened: breast cancer, ovarian cancer, colon cancer, clear cell renal cell carcinoma (RCC), uterine corpus endometrial carcinoma (UCEC), and lung adenocarcinoma (LUAD).

Gene expression analysis using human protein atlas

The Human Protein Atlas (HPA) database was utilized to obtain the expression data of FASN in different cells, tissues, and plasma. The data for plasma samples were estimated via mass spectrometry-based proteomics in the HPA database. "Low specificity" was defined by "Normalized expression ≥1 in at least one tissue/cell type, but not elevated in any tissue/cell type."

Immunohistochemistry (IHC) images of FASN in five pairs of normal and tumor tissues, including breast invasive carcinoma (BRCA), cervical squamous cell carcinoma and endocervical adenocarcinoma (CESC), colon adenocarcinoma (COAD), liver hepatocellular carcinoma (LIHC), and prostate adenocarcinoma (PRAD) were downloaded from the HPA and analyzed.

Gene expression analysis using Oncomine

We collected the different expression results of FASN between the tumor group and the corresponding normal group (P = 0.05, fold change = 1.5). Pooling analysis was performed across five comparisons. The median rank for FASN across each of the analyses, the P-value for the median-ranked analysis, and the legends of the enrolled studies were obtained.

Survival prognosis analysis

We utilized the Kaplan-Meier "Survival Map" module (GEPIA2) [15] to obtain the overall survival (OS) and disease-free survival (DFS) map of FASN. The expression threshold for splitting the high/low expression groups was 50%. The Kaplan-Meier survival analysis module of GEPIA2 was used to obtain survival plots using the log-rank test.

The interface of the Kaplan-Meier plotter was used to pool the different GEO datasets for a series of analyses of OS, distant metastasis-free survival (DMFS), relapse-free survival (RFS), post-progression survival (PPS), first progression (FP), disease-specific survival (DSS), and progression-free survival (PFS). The cases of lung, ovarian, lung, gastric, and liver cancers were split into two groups by setting "autoselect best cutoff." The hazard ratio (HR), 95% confidence intervals, and log-rank P-value were calculated, and Kaplan-Meier survival plots were generated. Clinical factors (e.g., histology, sex, smoking history, or chemotherapy) were also selected for a series of subgroup analyses.

Based on STATA 15.1 software (StataCorp LLC, College Station, TX, USA), we used the Kaplan-Meier function to perform a meta-analysis to pool the survival data of FASN.

Genetic alteration analysis

We collected the genetic alteration features, alteration frequency, mutation type, copy number alteration (CNA), mutated site information, and three-dimensional (3D) structure from the cBioPortal web [17, 18]. The OS, DFS, and PFS for the tumors with or without FASN genetic alterations were collected. Log-rank P-value was obtained and Kaplan-Meier analysis was performed.

Correlation of FASN and tumor mutational burden (TMB)/microsatellite instability (MSI)

TMB and MSI were obtained from the article, The Immune Landscape of Cancer and the Landscape of Microsatellite Instability Across 39 Cancer Types. The rank sum test detected two sets of data (p = 0.05). Spearman correlation was used to compare TMB/MSI and FASN gene expression.

DNA methylation analysis

We utilized the MEXPRESS web with the query "FASN" to obtain the DNA methylation status of FASN of various probes (e.g., cg06234966, cg24715260) in glioblastoma (GBM). The beta value of each sample, and the Benjamini-Hochberg-adjusted *P*-value and Pearson correlation coefficient (R) values were obtained.

We used the GSE50923 dataset [19] to assess the methylation status in 54 GBM tissues and 24 normal brain tissues. Briefly, the "minfi" R package and boxplot were employed to perform normalization. The mean methylation level of FASN and the normalized beta value of each sample at the selected methylation probes (cg03386722 and cg23244421) were visualized using the ggviolin function of the ggpubr package, with the setting, stat_compare_means (paired = T, method = "wilcox.test").

Phosphorylation feature prediction

We used the open-access PhosphoNET database to obtain the predicted phosphorylation features of the S207, S724, S725, T976, S1174, S1411, S2198, and T2204 sites by searching the protein name "FASN."

Immune infiltration analysis

The TIMER2 web server was used to explore the association between FASN expression and immune infiltrates. Immune cells of $CD8^+$ T-cells, $CD4^+$ T-cells, cancer-associated fibroblasts, and NK cells were screened. Purity-adjusted Spearman's rank correlation test was used to obtain *P*-values and partial correlation (cor) values.

FASN-related gene enrichment analysis

The STRING website was utilized to obtain FASN-binding proteins, as demonstrated by experiments. The low confidence score was set as 0.150. Further, maximum number of interactors ≤50, physical interaction, and evidence were the basis of the interaction types.

The top 100 FASN-correlated targeting genes were obtained using the "Similar Gene Detection" module (GEPIA2). The pairwise gene correlation of FASN and the selected genes was obtained using the "correlation analysis" module. Moreover, a heatmap of the screened genes was obtained with the "Gene_Corr" module. Purity-adjusted Spearman's rank correlation test was used to obtain *P*-values and partial correlation (cor) values.

We conducted Kyoto Encyclopedia of Genes and Genomes (KEGG) pathway analysis with the two sets of data. Database for Annotation, Visualization, and Integrated Discovery (DAVID) was utilized to acquire the functional annotation results. The enriched pathways were finally visualized with the "tidyr" and "ggplot2" R packages. Gene ontology (GO) enrichment analysis was also conducted with the "clusterProfiler" R package (Two-tailed $P < 0.05$).

Data availability

The datasets analyzed in this study can be found in the online dataset. Requests for further access to the dataset can be directed to hxl950513@126.com.

Highlights

A pan-cancer analysis of FASN. FASN is differentially associated with the prognosis of different tumor cases. The link between FASN and $CD8^+$ T-cells, $CD4^+$ T-cells, cancer-associated fibroblast infiltration, and NK cells. Enhanced phosphorylation level of S207 in several tumors, such as colon cancer. Hormone receptor binding- and fatty acid metabolic process-associated issues are involved in the cancerous role of FASN.

RESULTS

Gene mapping and protein structure analysis

In this study, we investigated the oncogenic function of FASN (NM_004104 or NP_004595.4, Supplementary Figure 1A). The protein structure of FASN is conserved among various species (e.g., *H. sapiens*, *G. gallus*, *C. elegans*) and generally involves the cond_enzymes (cl09938) domain and acyl_transf_1 (cl08282) domain (Supplementary Figure 1B). A phylogenetic tree (Supplementary Figure 2) revealed the evolutionary relationship of the FASN protein across various species.

Gene expression analysis

The expression level of FASN in various cells/nontumor tissues/plasma was determined. FASN

had the highest expression in the adipose tissue, followed by the breast and liver (Figure 2A). FASN was identified in all tissues, except granulocytes, and displayed tissue-enhanced (adipose tissue) RNA tissue specificity. Low RNA blood cell type specificity was demonstrated in various blood cells (Figure 2B). The protein density of FASN in the plasma was 1.6 μg/L, which might be due to the biological external leakage of the intracellular compound (Figure 2C).

We analyzed the expression status of FASN in cancers. The expression level of FASN in the tissues of bladder urothelial carcinoma (BLCA), COAD, LIHC, PRAD, READ (Rectum adenocarcinoma), Stomach adenocarcinoma (STAD), Uterine Corpus Endometrial Carcinoma (UCEC) ($P < 0.001$), CESC, esophageal carcinoma (ESCA), head and neck squamous cell carcinoma (HNSC), kidney renal papillary cell carcinoma (KIRP) ($P < 0.01$), and kidney renal clear cell carcinoma (KIRC) ($P < 0.05$) was greater than that in comparable tissues (Figure 3A).

By incorporating the GTEx dataset, the expression level between the tumor-normal pair tissues was further identified in BLCA, CESC, COAD, lymphoid neoplasm diffuse large B-cell lymphoma (DLBC), LIHC, ovarian serous cystadenocarcinoma (OV), pancreatic adenocarcinoma (PAAD), PRAD, READ, testicular germ cell tumors (TGCT), thymoma (THYM), UCEC, and uterine carcinosarcoma (UCS) (Figure 3B, $P < 0.05$). However, a significant difference was not found for other tumors, such as ESCA, HNSC, LGG (brain lower grade glioma), or SARC (sarcoma) (Figure 4A).

Increased FASN expression was found in colon cancer and UCEC (Figure 3C, $P < 0.001$) relative to comparable tissues from the CPTAC dataset. The results of the pooling analysis (Figure 5) further

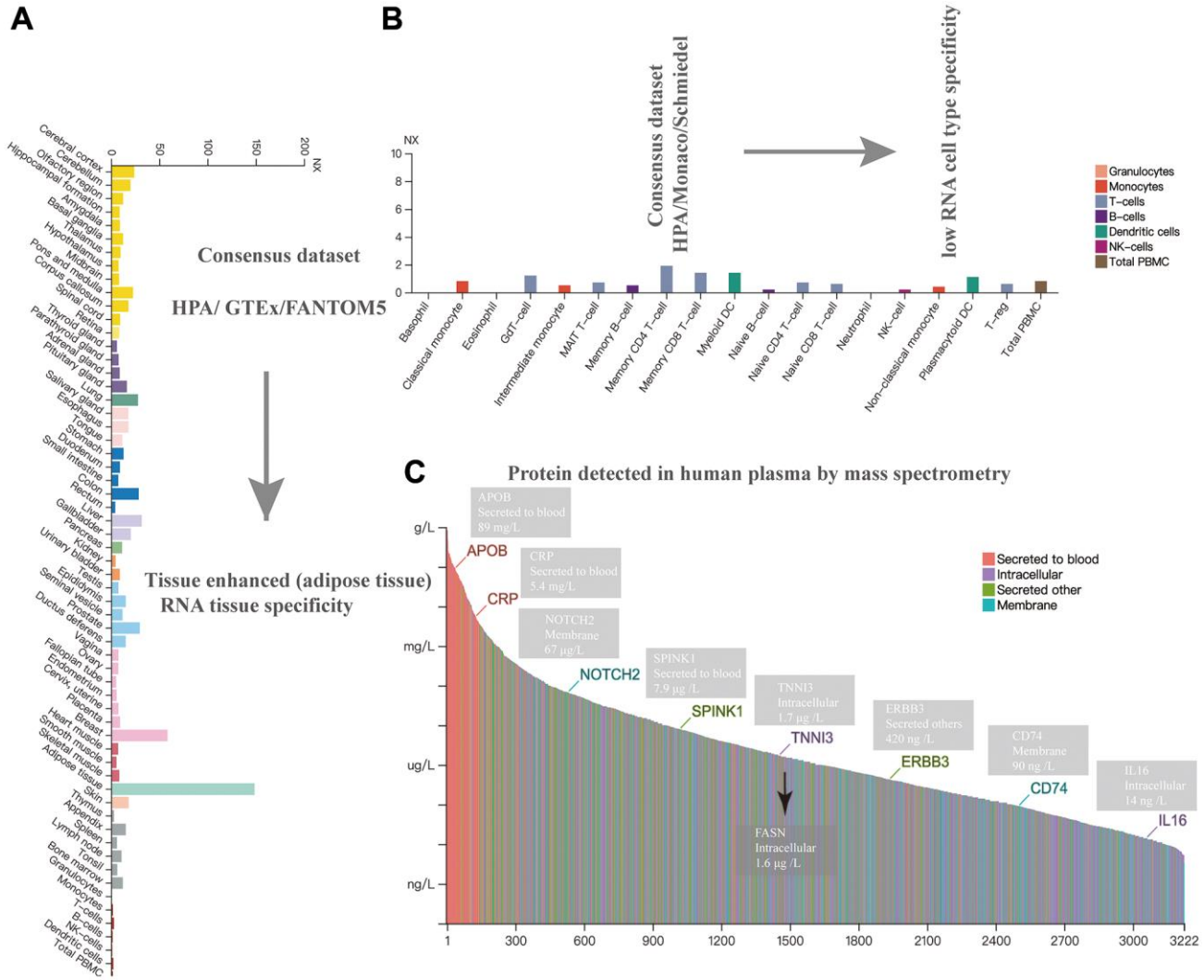

Figure 2. Expression analysis of FASN in different cells, tissues, and plasma. Expression of the *FASN* gene in different tissues (**A**), blood cells (**B**), and plasma (**C**) based on mass spectrometry.

affirmed that FASN expression was higher in bladder cancer, colorectal cancer, lymphoma, ovarian cancer, and prostate cancer tissues (P < 0.001) than in corresponding normal controls. A correlation was also found between FASN expression and the pathological stages of CESC, KICH, KIRC, KIRP, OV, READ, and thyroid carcinoma (THCA) (Figure 3D, P < 0.05); however, no correlation was found for other tumors (Figure 4B–4E).

Immunohistochemistry analysis

The IHC results were obtained and the results of FASN gene expression in tumor tissues were compared with

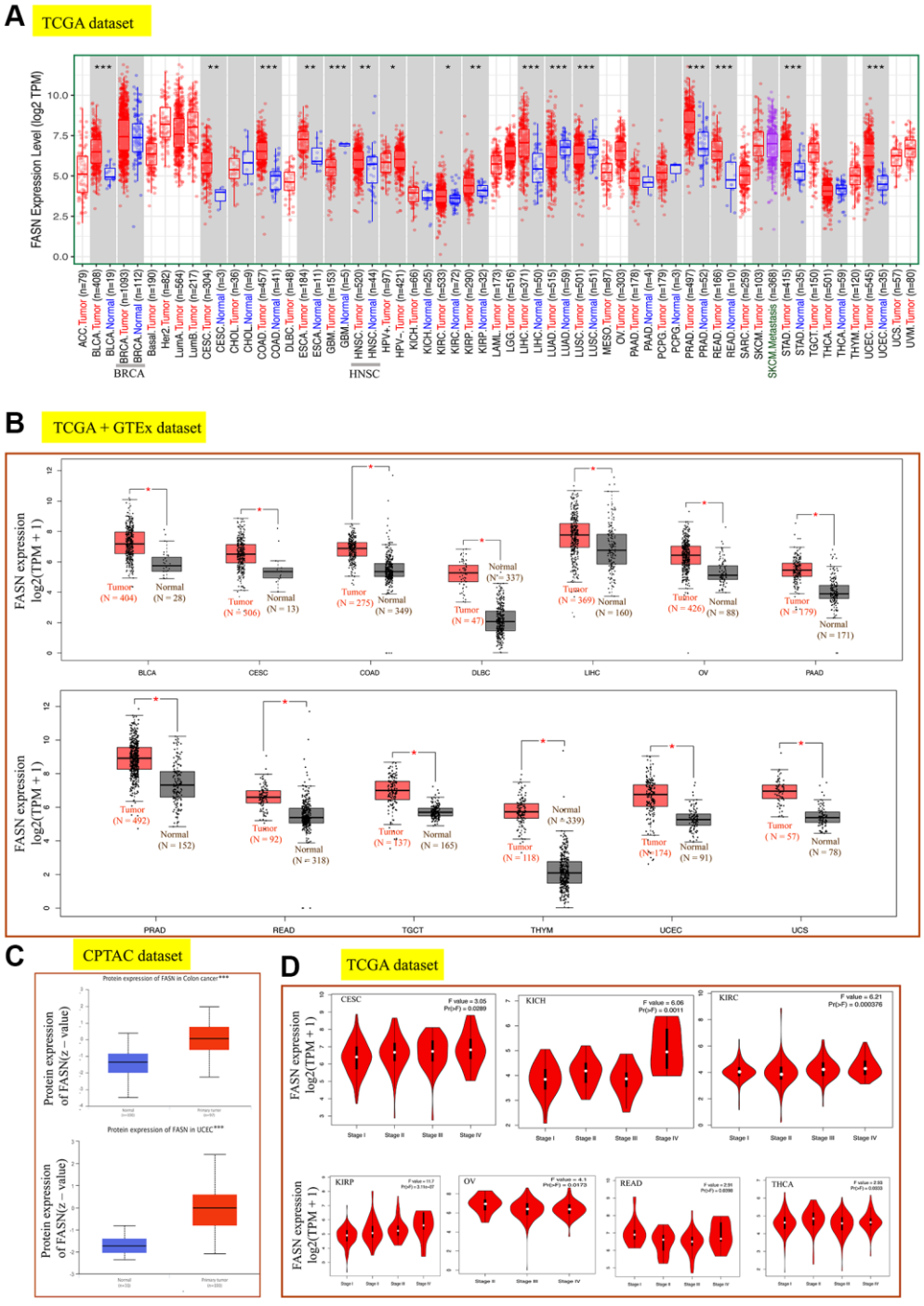

Figure 3. Expression analysis of the *FASN* gene across various tumors and pathological stages. (**A**) Expression analysis of the *FASN* gene in various cancers. (**B**) After employing the GTEx database, the box plot data were retrieved. (**C**) Expression analysis of FASN total protein between the normal group and the colon cancer and UCEC group. (**D**) Expression analysis of the *FASN* gene was performed according to the pathological stages. $^{*}P < 0.05$; $^{**}P < 0.01$; $^{***}P < 0.001$.

those in normal tissues. The gene expression data were found to be consistent with those of IHC. Negative or low IHC staining was obtained in the normal breast, cervix, colon, liver, and prostate tissue, while medium or strong staining was obtained in the cancer tissue (Figure 6).

Survival analysis data

We explored the relationship between FASN expression and the outcome of patients in the high and low expression groups. As shown in Figure 7A, high expression of FASN was related to poor OS outcomes

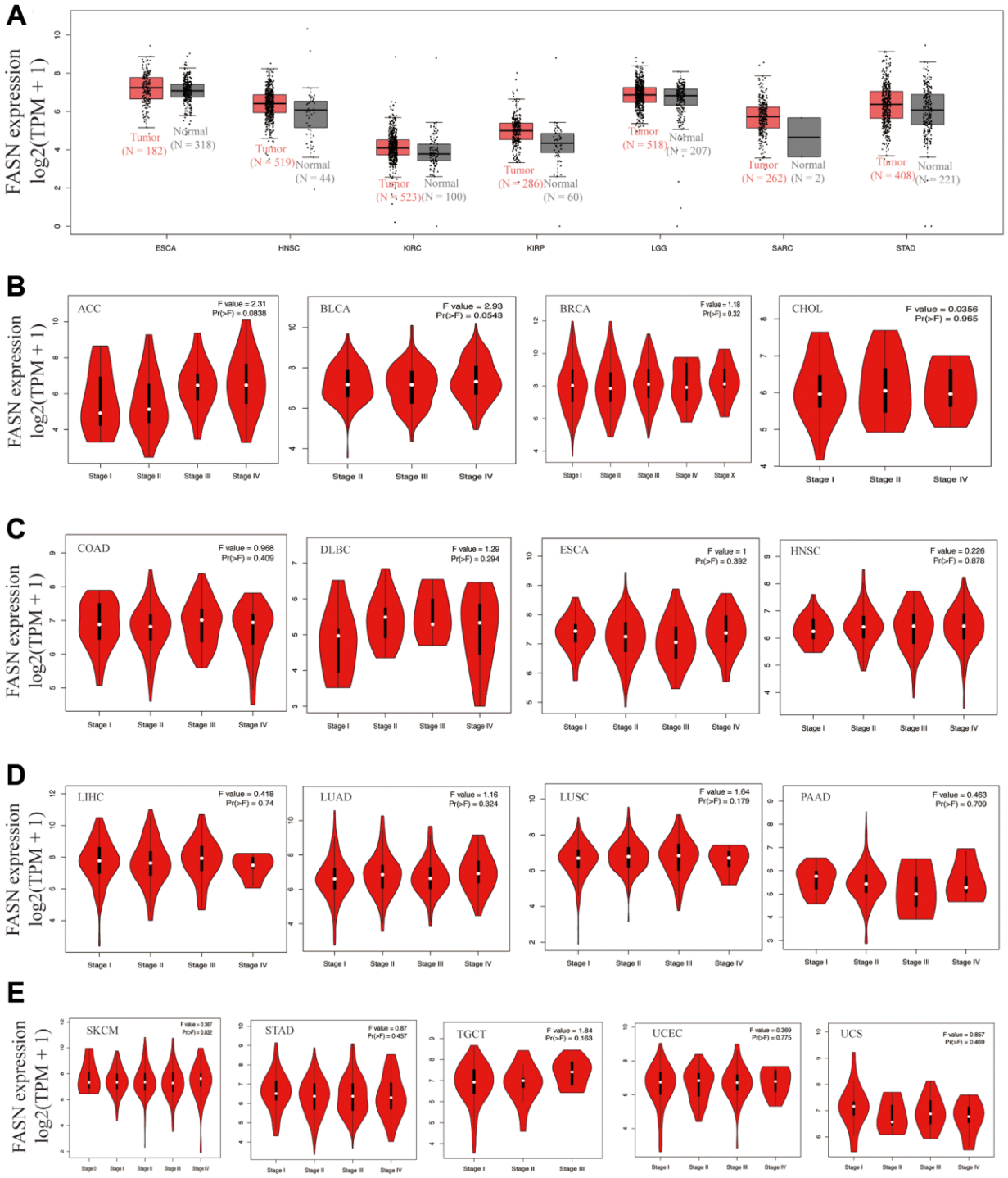

Figure 4. Expression analysis of the *FASN* gene across various tumors and pathological stages. (**A**) Expression analysis of the *FASN* gene in ESCA, HNSC, KIRC, KIRP, LGG, SARC, and STAD based on the GTEx databases. Expression analysis of the different pathological stages of ACC, BLCA, BRCA, CHOL (**B**); COAD, DLBC, ESCA, HNSC (**C**); LIHC, LUAD, LUSC, PAAD (**D**); and SKCM, STAD, TGCT, UCEC, UCS (**E**).

in ACC (p = 0.015), BLCA (p = 0.0044), CESC (p = 0.004), HNSC (p = 0.045), KIRC (p = 3.9e-06), KIRP (P = 0.017), MESO (Mesothelioma) (P = 0.0043), LGG (P = 0.0035), and SARC (P = 0.018). DFS analysis (Figure 7B) further revealed a relationship between high FASN expression and poor outcome of ACC (p = 0.015), CESC (p = 0.023), LGG (p = 0.028), and KIRP (p = 0.02).

The Kaplan-Meier plotter tool revealed that FASN was associated with poor RFS (P = 0.0093) outcome for ovarian cancer (Figure 8A) and poor OS (P = 1e-08), FP (P = 1.2e-06), and PPS (P = 0.019) prognosis for lung cancer (Figure 8B). Additionally, a high FASN level was found to have a significant effect on the poor OS (P = 1.6e-16), FP (P = 1.8e-13), and PPS (P < 1e-16) outcomes for gastric cancer (Figure 8C). In contrast, a significant relationship between low expression of FASN and poor OS (P = 0.018), poor RFS (P = 3.5e-06), poor DMFS (P = 5.7e-05), and poor PPS (P = 0.022) outcomes was found for breast cancer (Figure 8D). In fact, a high expression of FASN was associated with poor OS, RFS, DMFS, and PPS (Supplementary Table 1, P < 0.05) for breast cancer patients with HER2 negative. Although we carried out further studies of liver cancer, a significant relationship between FASN and OS, PFS, RFS, and DSS outcomes was not found (Figure 8E, P < 0.05). Nonetheless, the results of the meta-analysis (Figure 9) confirmed the significant relationship between FASN expression and the outcomes for breast cancer, liver cancer, lung cancer, and gastric cancer (P < 0.05) but not for ovarian cancer (P = 0.998). Subgroup analyses were also performed with the clinical characteristics and definite results were

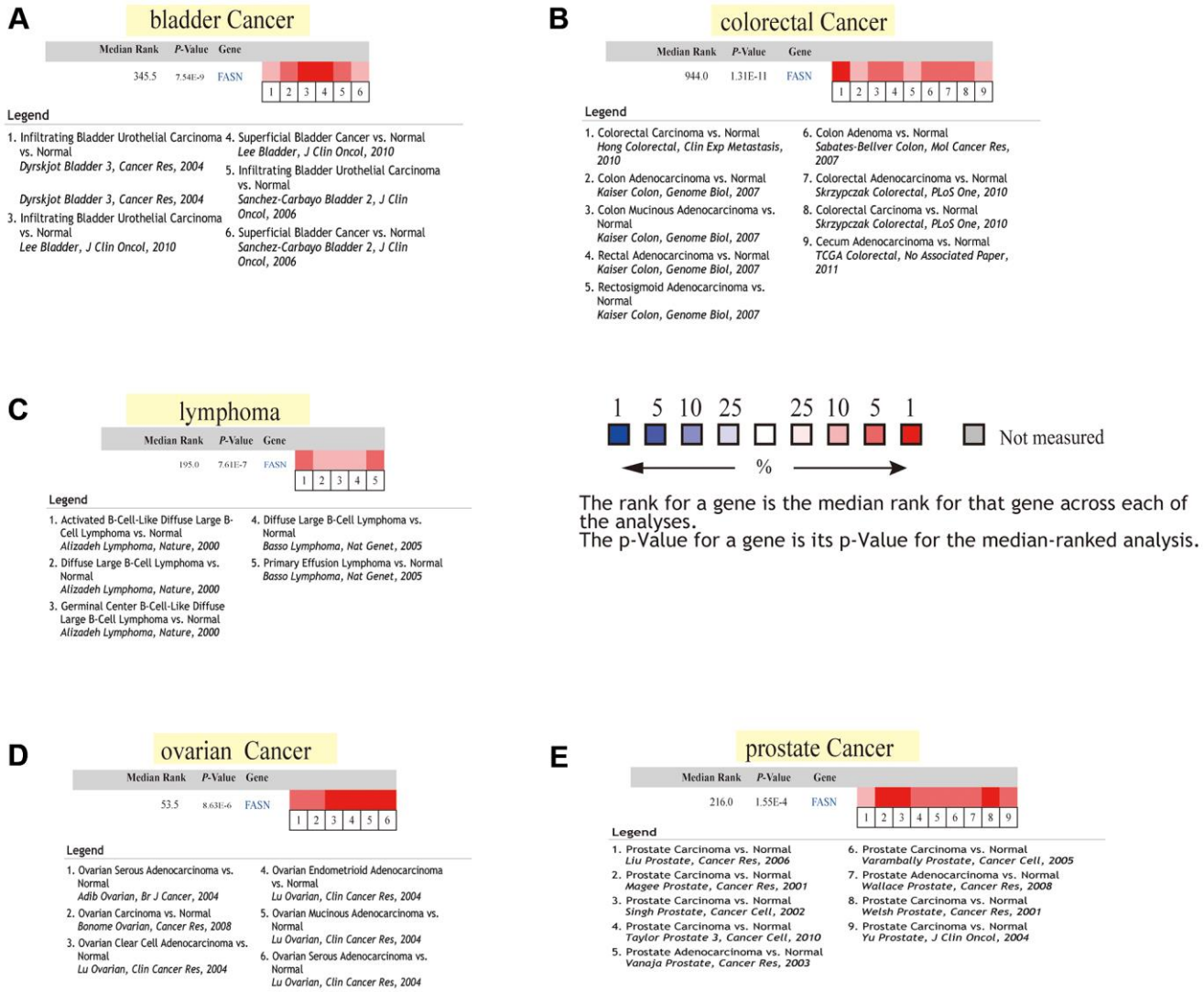

Figure 5. Pooled FASN analysis using normal and tumor tissues. (**A**) Lung cancer; (**B**) kidney cancer; (**C**) colorectal cancer; (**D**) lymphoma; and (**E**) myeloma.

obtained (Supplementary Tables 1–5). Overall, the findings revealed that FASN is dissimilarly associated with the outcome of cancer cases.

Genetic alteration analysis

The genetic alteration level of FASN has been observed in various cancers. The highest alteration frequency of FASN (>11%) was found in patients with Skin Cutaneous Melanoma with "mutation" (Figure 10A). The CNA data of liver HCC showed a >5% alteration incidence (Figure 10A). However, the value in thymoma cases (~1% genetic alteration frequency) was not detected (Figure 10A). Figure 10B shows the types, sites, and number of FASN genetic alterations. The missense mutation of FASN is the principal type of

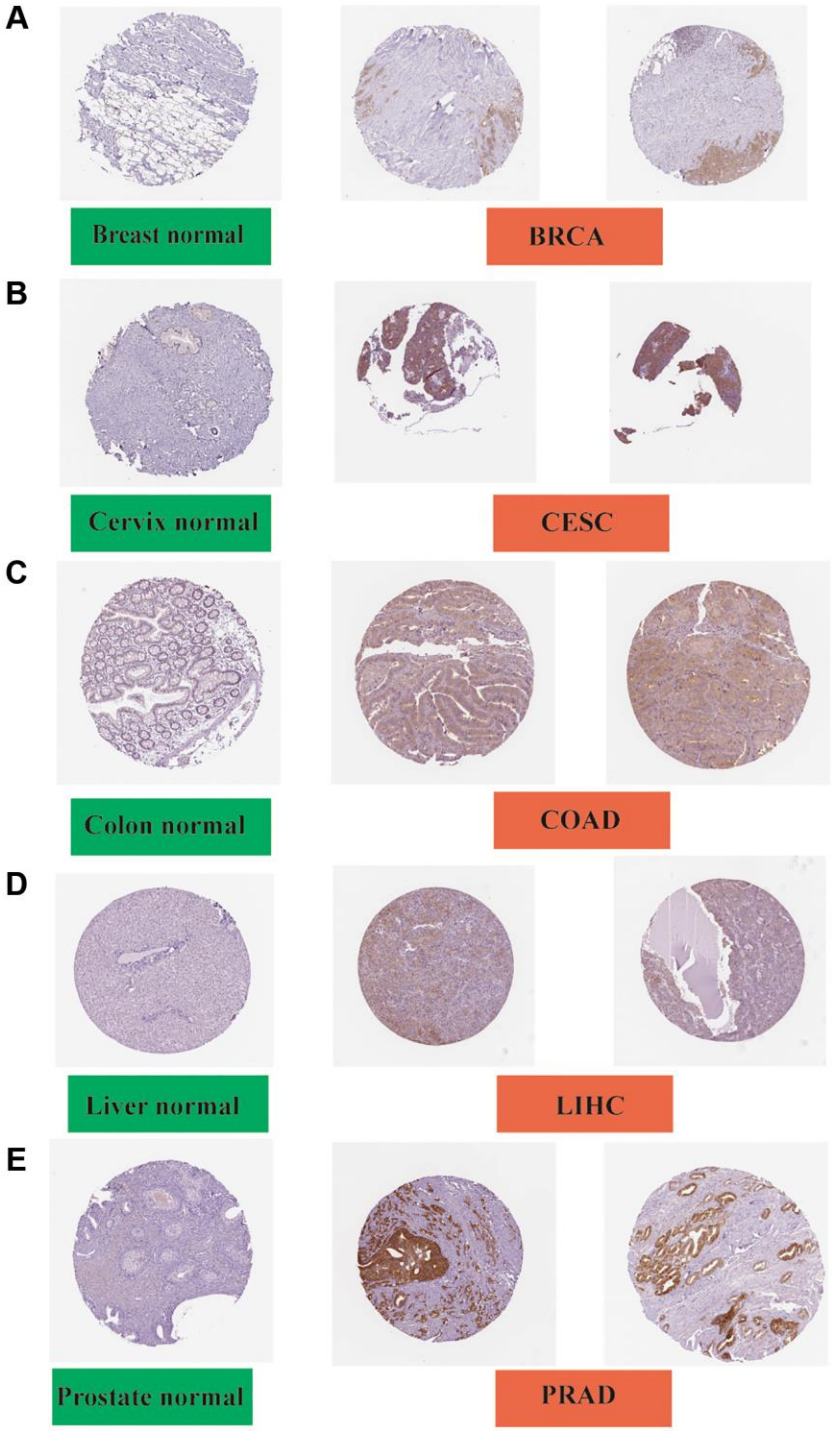

Figure 6. Immunohistochemistry slides of normal (left) and tumor (middle and right) tissues. FASN protein expression was significantly higher in BRCA, CESC, COAD LIHC, and PRAD. (**A**) Breast; (**B**) Cervix; (**C**) Colon; (**D**) Liver; and (**E**) Prostate.

genetic alteration. L1353Sfs*20 alteration (four cases of uterine endometrioid carcinoma and one case of stomach adenocarcinoma) between Methyltransf_12 and ADH_zinc_N could induce a translation mutation from L (leucine) to S (serine) at the 1353 site of the FASN protein (Figure 10B). The L1353 locus was identified in the 3D protein structure (Figure 10C). Moreover, the relationship between genetic alterations and clinical outcomes of cancers was investigated.

Figure 10D shows that MESO patients with altered FASN had better outcomes for OS (P = 0.0248), but not for PFS (P = 0.209) while STAD patients had better OS (P = 0.602) and PFS (P = 0.392) than patients without FASN alteration.

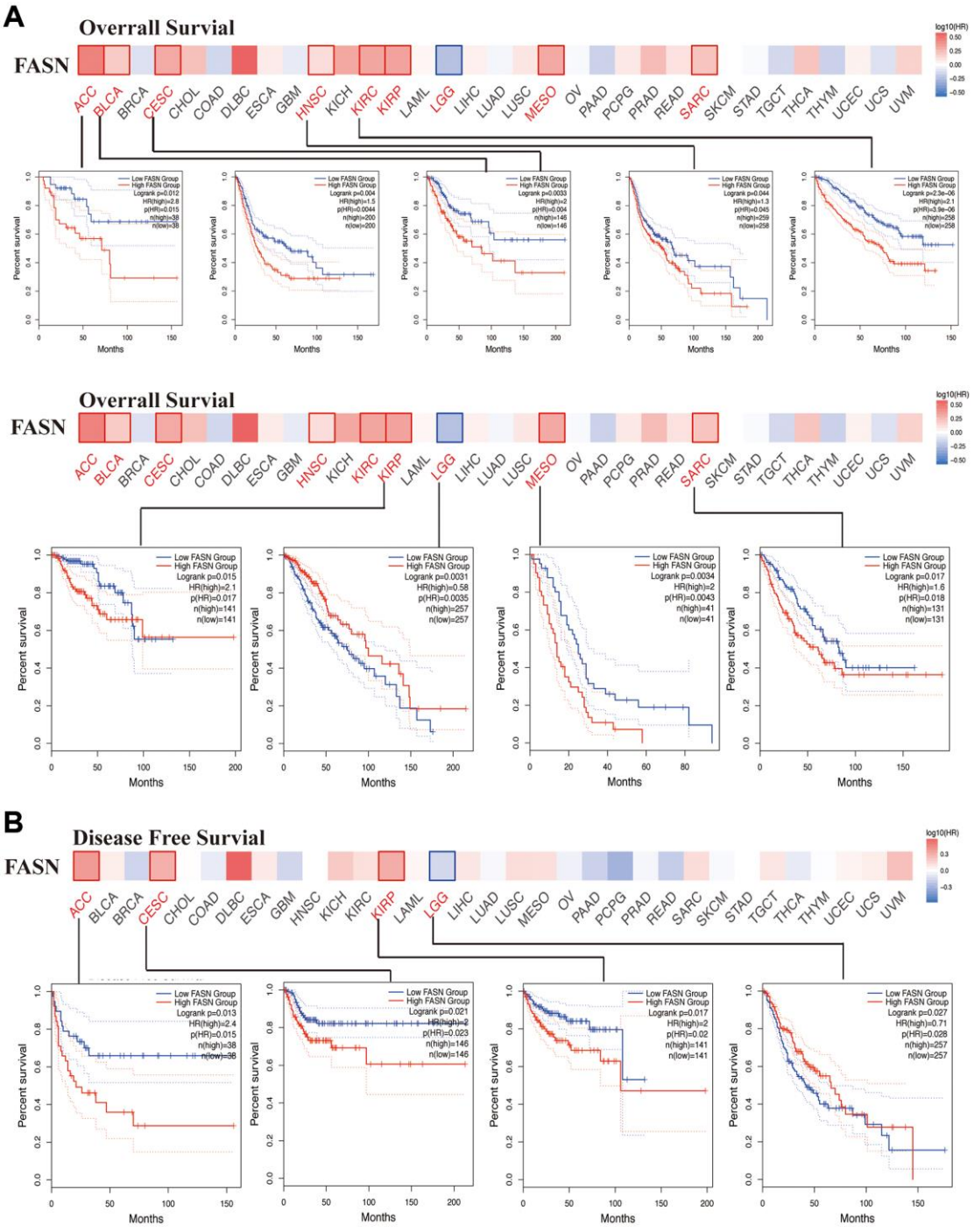

Figure 7. Correlation between FASN gene and the survival outcome of tumors. OS (**A**) and DFS (**B**) analyses of various tumors. The survival map and Kaplan-Meier curves with positive results are displayed.

TMB/MSI analysis

The correlation between FASN expression and TMB/MSI was determined. An adverse significant association was found between FASN and TMB for STAD, HNSC, UCEC, LUAD, LIHC, KICH, READ, THYM, PRAD, ACC, SARC, and BLCA, while a significant association was found for BRCA, LGG, and THCA (Figure 11). With respect to MSI, DLBC, READ, PCPG, THCA, HNSC, and BRCA were found to have a significant negative correlation, while CESC, LUAD, UCEC, KIRC, SARC (Sarcoma), GBM, TGCT,

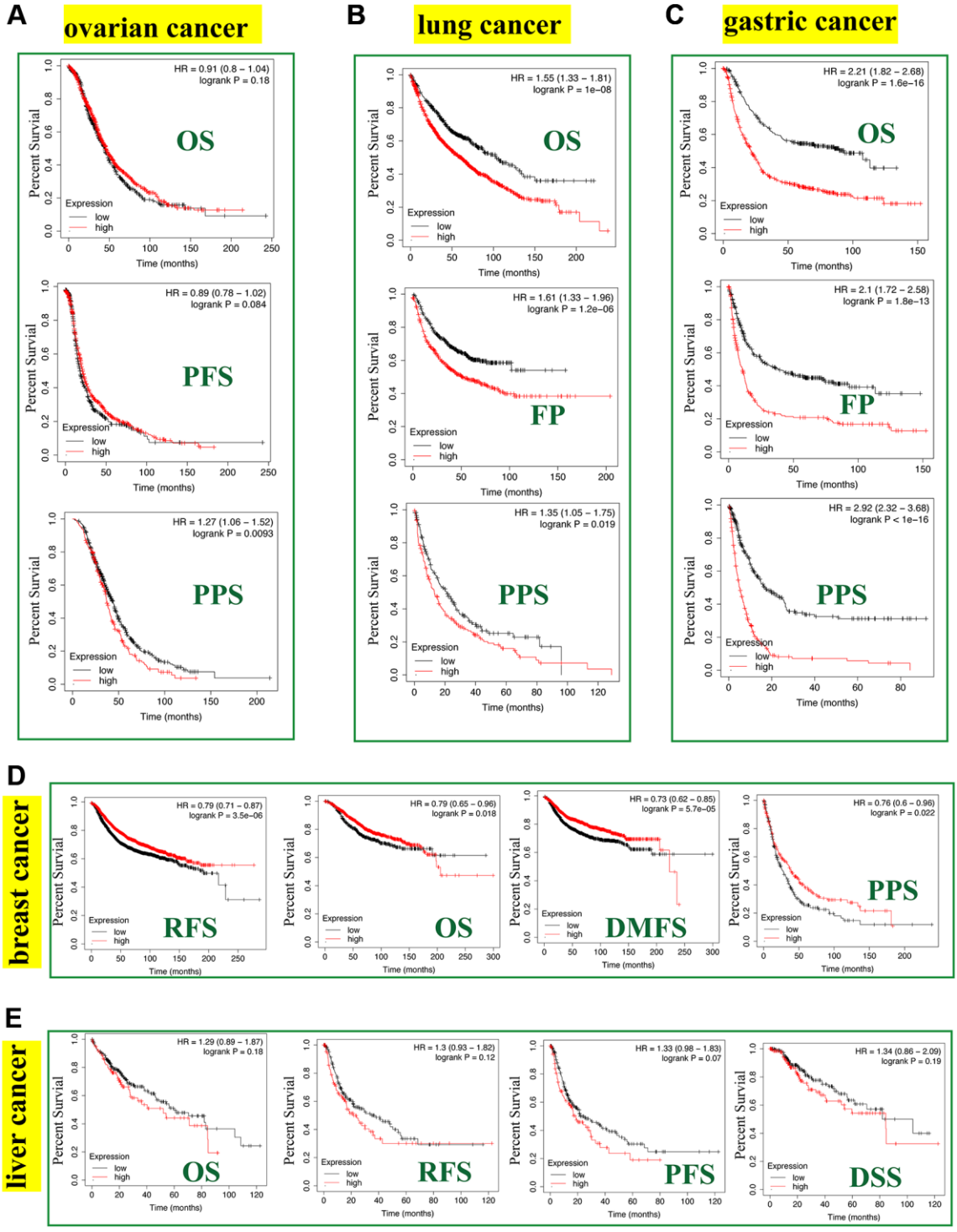

Figure 8. Correlation between the *FASN* gene and the survival outcome of tumors. We used the Kaplan-Meier plotter to carry out the survival analyses of *FASN* gene in breast cancer (**A**), ovarian cancer (**B**), lung cancer (**C**), gastric cancer (**D**), and liver cancer (**E**) cases.

STAD, UVM, and LUSC had a significant positive correlation (Figure 12). More studies are required to explain this phenomenon.

DNA methylation analysis

We investigated the correlation between FASN DNA methylation and tumorigenesis in various cancers. With respect to GBM, we obtained a significant adverse relationship between DNA methylation and gene expression at probes of the non-promoter region, such as cg06234966 (P < 0.01, R = 0.322) (Figure 13). The GSE50923 dataset was used to confirm these results. In light of the standard methylation result (Figure 14A), we neglected the difference between GBM tissues and normal tissues (Figure 14B, P = 2.06e-06). Furthermore, we observed a decrease in the methylation level of FASN in cancer tissue compared to normal tissue for the selected probes (Figure 14C, cg03386722, P = 1.34e-06, Figure 14D, cg23244421, P = 0.03).

Protein phosphorylation analysis

FASN phosphorylation levels between normal tissues and the corresponding tumor group were obtained, and six types of cancers (breast cancer, clear cell RCC, LUAD, ovarian cancer, colon cancer, and UCEC) were analyzed. Figure 15A summarizes the FASN phosphorylation sites among these cancers.

The S207 sites within the ketoacyl-synt domain of FASN showed significant difference phosphorylation levels in tumor tissue compared to normal tissue (Figure 15B–15D, Figure 15F–15H, all P < 0.05), followed

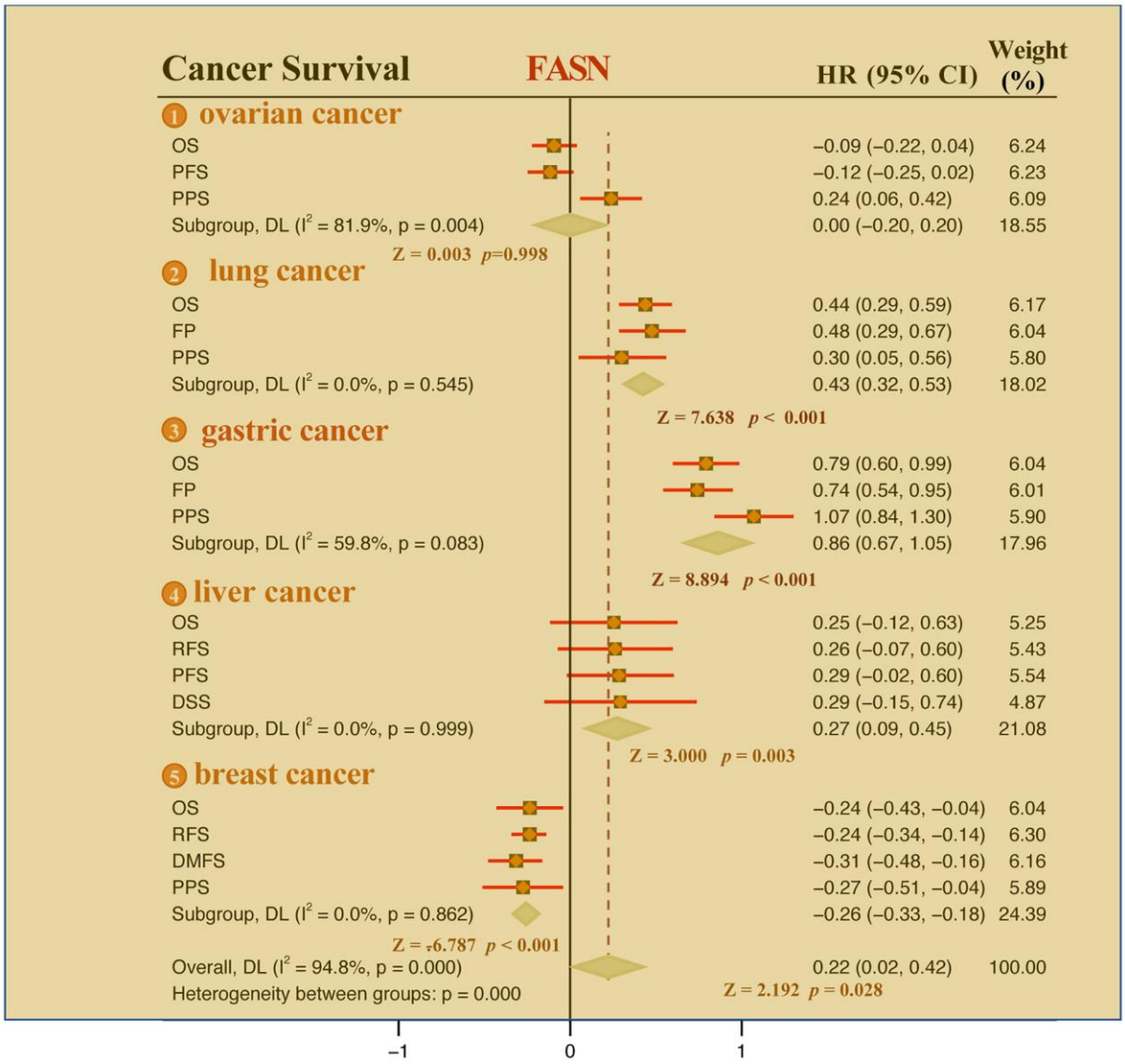

Figure 9. Meta-analysis of the correlation between FASN and the outcomes of breast cancer, ovarian cancer, lung cancer, gastric cancer, and liver cancer cases.

by the T2204 sites between PP-binding and thioesterase domain for colon cancer (Figure 15B, P = 5.8e-10), UCEC (Figure 15C, P = 8.0e-04) and breast cancer (Figure 15E, P = 1.9e-03). The PhosphoNET database revealed that FASN phosphorylation of S207 in the molecular responses to pathway activation was experimentally supported by previous investigations [20, 21] (Supplementary Table 6). Such finding aided in the exploration of the cancer role of S207 phosphorylation in tumors.

Immune infiltration analysis

Tumor-infiltrating immune cells can enhance the development, progression, or metastasis of cancers [22, 23]. A statistically significant adverse relationship was found between $CD8^+$ T cells and FASN expression in HNSC, KIRC, OV, and SARC (Figure 16), depending on all/most algorithms. Further, a statistically significant relationship was presumed between FASN expression and cancer-associated fibroblasts for CESC, KIRC, KIRP, OV, and UVM; however, a negative correlation was presumed for LGG, PRAD, and STAD (Figure 17). A negative correlation was also found between FASN expression and CD4+ T cells and NK cells in BLCA, BRCA, and THCA, while a positive correlation was found in HNSC (Supplementary Table 7).

Enrichment analysis of FASN-related partners

We screened out FASN-binding proteins and FASN-expression-correlated genes for functional enrichment

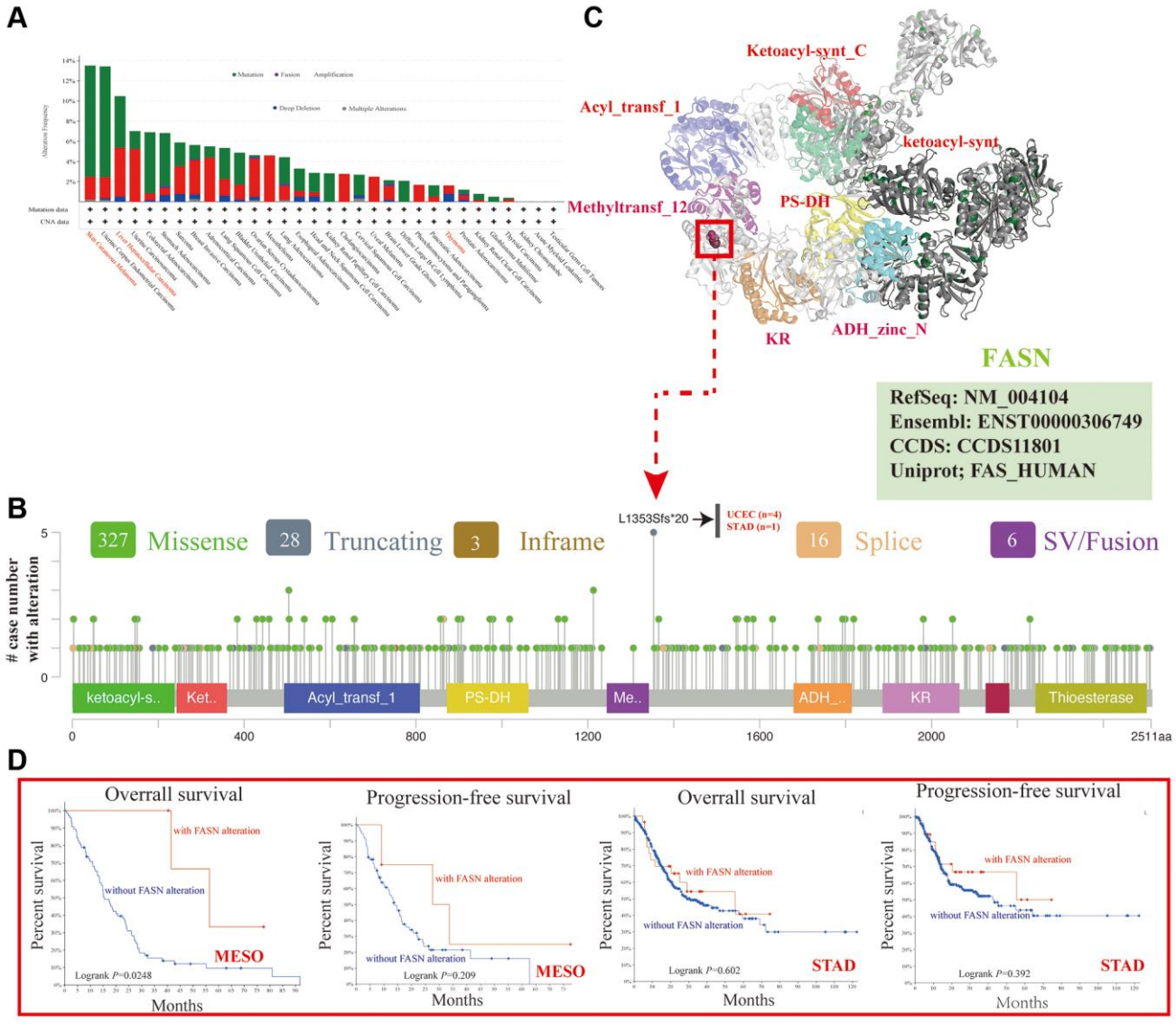

Figure 10. Mutation feature of FASN across various tumors. The alteration frequency with mutation type (**A**) and mutation site (**B**) is displayed. The mutation site with the highest alteration frequency (L1353Sfs*20) in the 3D structure of FASN (**C**). The potential correlation between mutation status and the OS and PFS of MESO and STAD (**D**).

analyses. We collected 51 FASN-binding proteins using the STRING tool (Figure 18A). FASN expression was positively associated with five genes. The top 100 FASN-correlated targeting genes included glycerol-3-phosphate acyltransferase, mitochondrial (*GPAM*) (R = 0.64), stearoyl-CoA desaturase (SCD) (R = 0.62), cell death inducing DFFA-like effector c (CIDEC) (R = 0.61), diacylglycerol O-acyltransferase 2 (DGAT2) (R = 0.58), and pyruvate carboxylase (PC) (R = 0.32) (P < 0.001) (Figure 18B). The heatmap revealed a positive

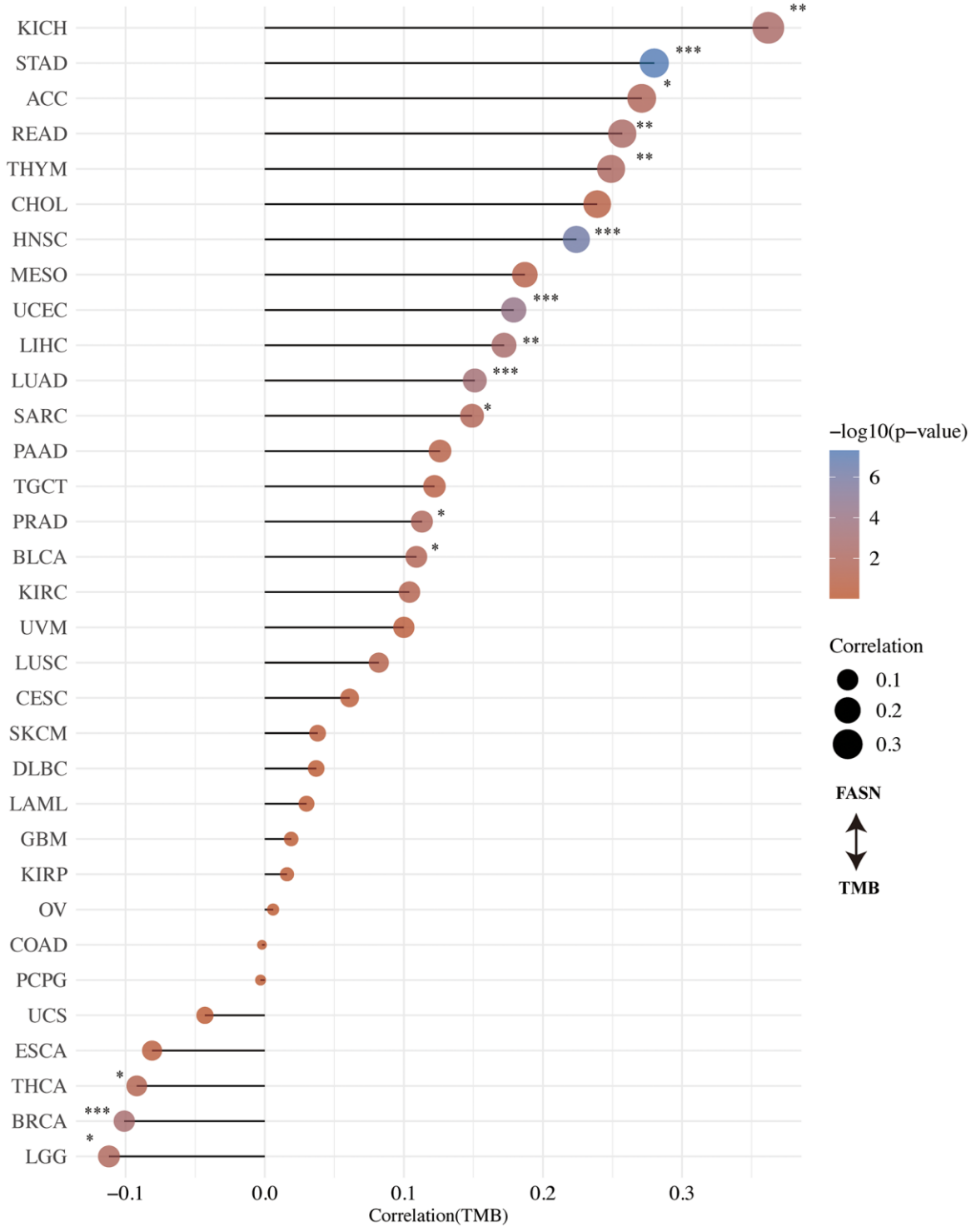

Figure 11. Correlation between FASN expression and tumor mutational burden.

correlation between FASN and the five genes across cancer types (Figure 18C). PC was the only intersection member of the two groups (Figure 18D).

The KEGG analysis resulted presented in Figure 18E revealed that "metabolic pathways" and "PPAR signaling pathway" might play a role in the effect of FASN on tumorigenesis. GO analysis further suggested that these genes were mainly enriched in lipid metabolism, such as triglyceride lipase activity, lipid droplets, fatty acid metabolic processes, regulation of lipid metabolic processes, and others (Figures 18F and 19).

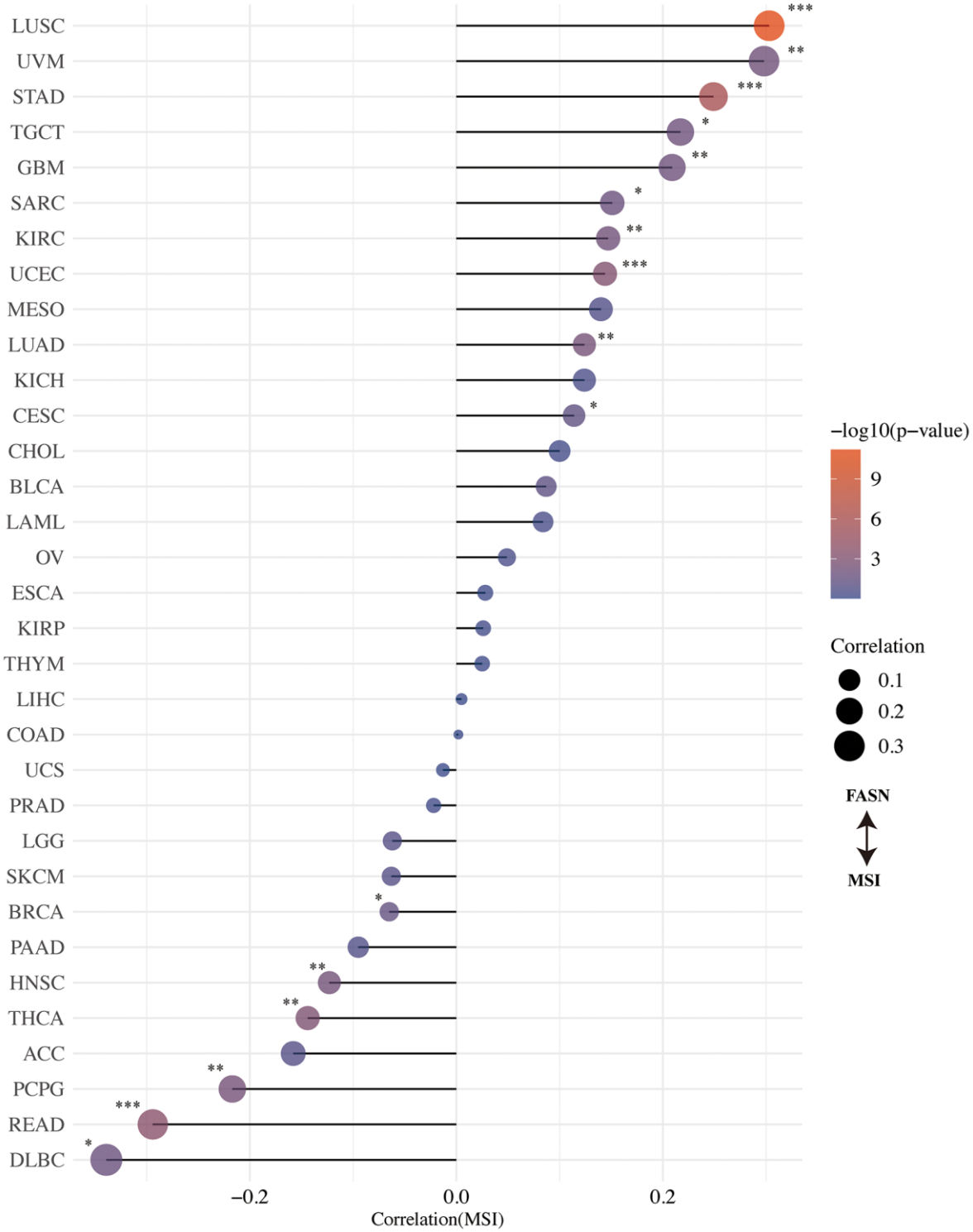

Figure 12. Correlation between FASN expression and microsatellite instability.

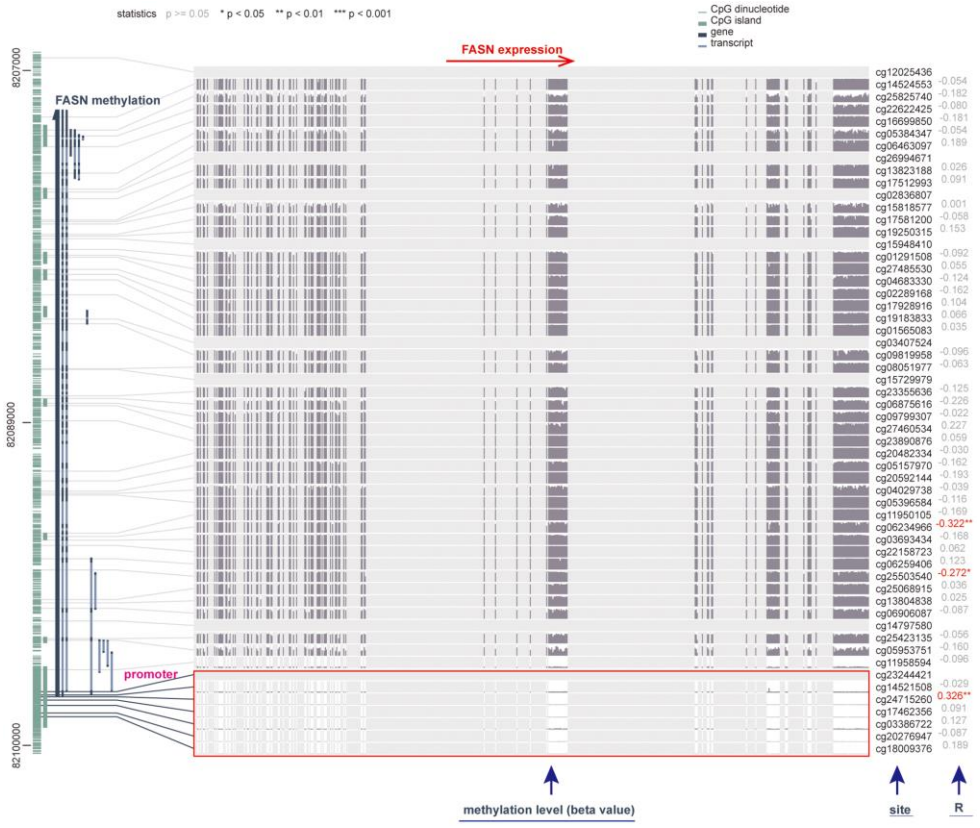

Figure 13. Correlation between DNA methylation and FASN expression in GBM cases. The promoter region is selected.

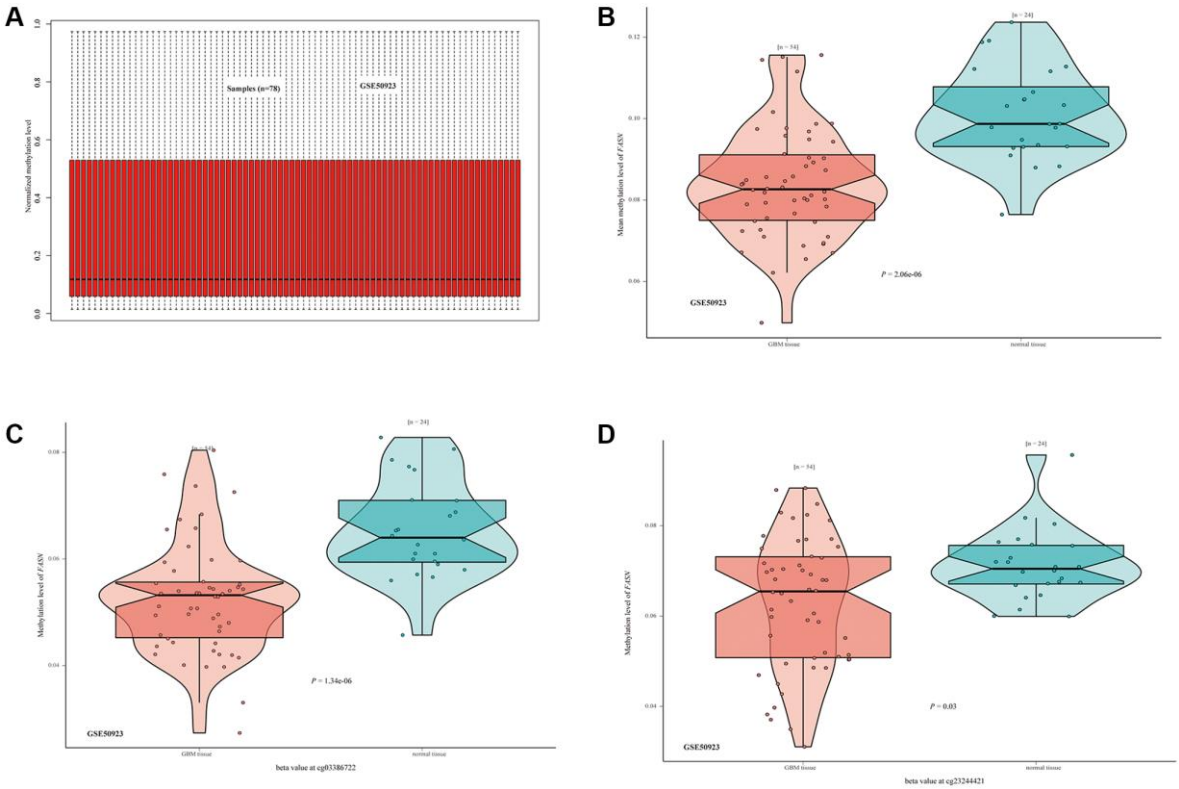

Figure 14. DNA methylation status of FASN in the GSE50923 dataset. (**A**) Normalization of the GSE50923 dataset; (**B**) methylation status of FASN in the GBM group and the matched normal group; (**C**, **D**) beta value of FASN in cg03386722 and cg23244421.

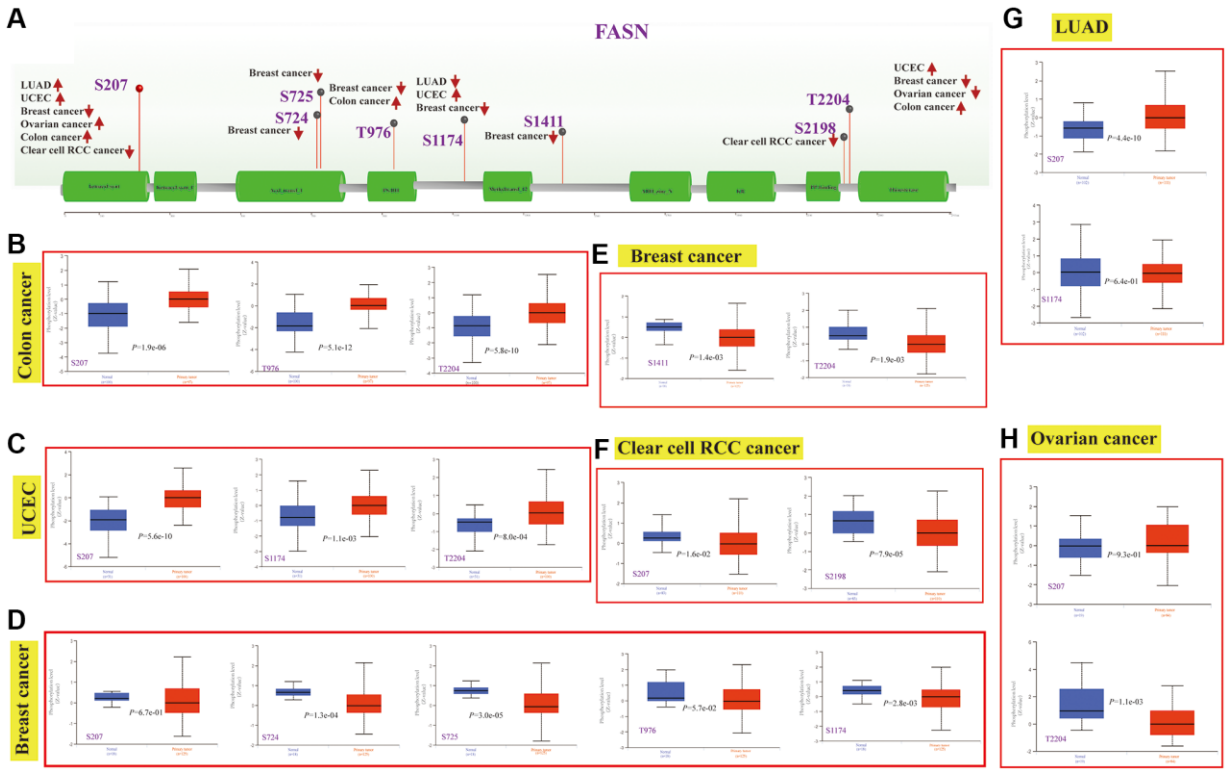

Figure 15. Phosphorylation analysis of the FASN protein. Phosphoprotein sites of the FASN protein are indicated in the schematic (**A**). Expression analysis of FASN phosphoprotein (NP_004595.4, S207, S724, S725, T976, S1174, S1411, S2198 and T2204 sites) between normal tissue and tumors, including colon cancer (**B**), UCEC (**C**), breast cancer (**D**, **E**), clear cell RCC (**F**), LUAD (**G**), and ovarian cancer (**H**).

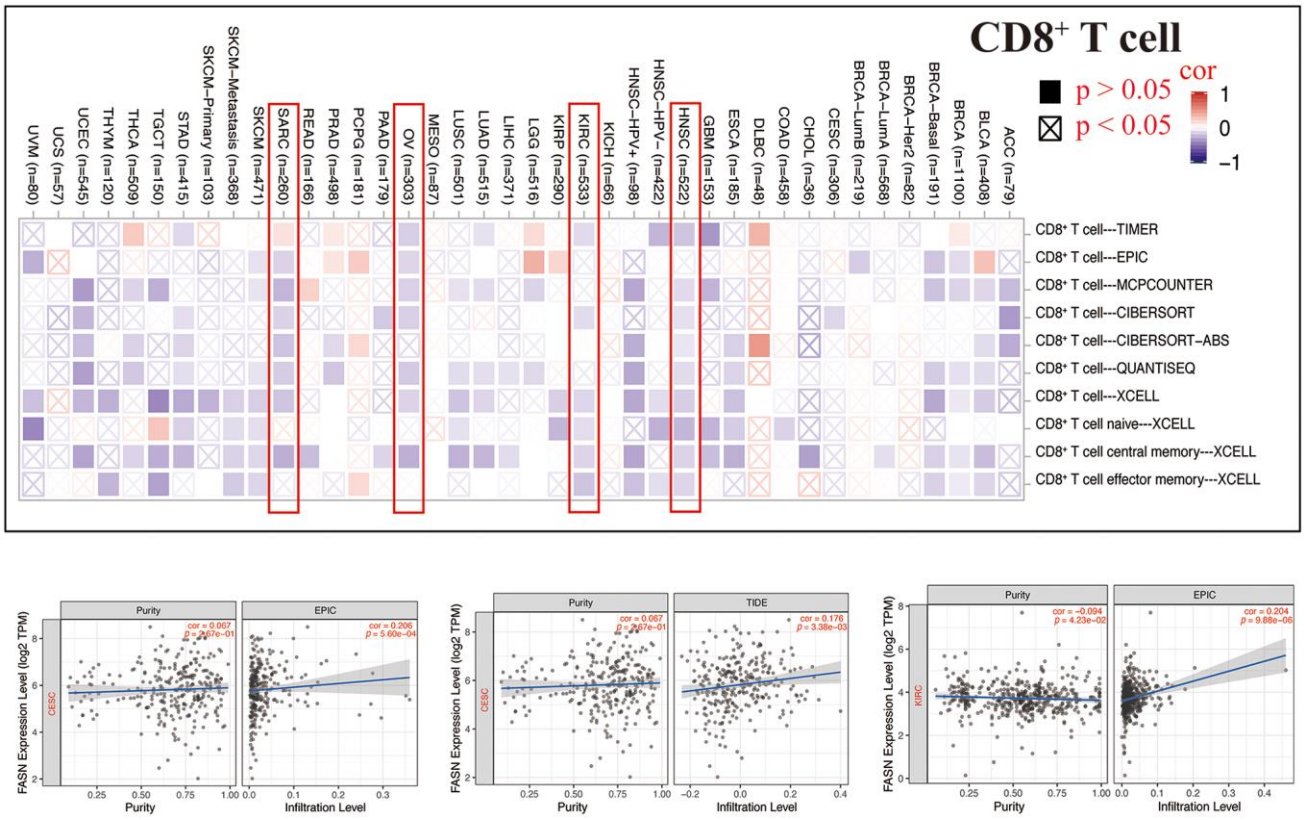

Figure 16. Relationship between FASN expression and CD8+ T-cells.

DISCUSSION

The FASN protein participates in multiple functions in biological processes across various species, such as gene axis, maturation of Treg cells, and cell apoptosis [24–26]. Several studies have revealed a functional connection between FASN and cancers. However, whether FASN can play a role in the tumorigenesis of cancers through these mechanisms remains unclear. Initially, the "HomoloGene" and phylogenetic tree suggested the conservation of the protein structure of FASN among various species, indicating that similar mechanisms may exist as a regular physiological role.

FASN expression was found to be higher in most tumor tissues than contrast tissues. However, survival outcome analysis yielded distinct conclusions for different tumors. Based on our analysis, FASN had a higher expression at the protein level in breast cancer. Based on prior studies, a high expression of FASN can increase the recurrence or metastasis rate of breast cancer [27–29]. Herein, high presentation was not found to be related to poor OS and DMFS outcomes in patients with breast cancer. However, high FASN expression was related to poor OS, RFS, DMFS, and PPS in breast cancer cases with HER2 negative subtype/mesenchymal (Supplementary Table 1). A recent study revealed that FASN has a higher expression in the HER2 positive subgroup than the HER2 negative group, and its inhibitor could prevent the agonistic tumor-promoting activity of tamoxifen and restore its estrogen antagonist properties against

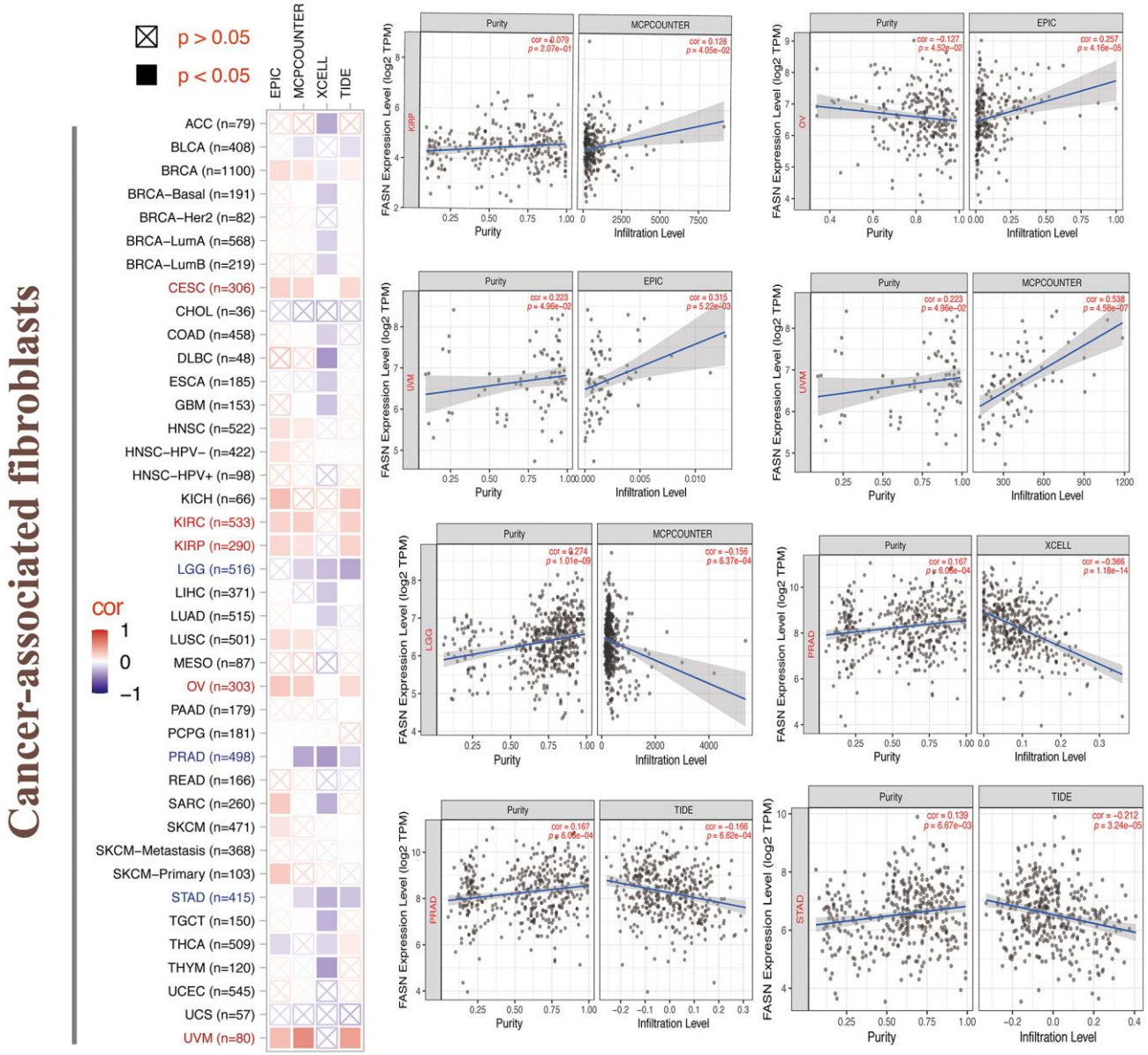

Figure 17. Relationship between FASN expression and cancer-associated fibroblasts.

ER/HER2- positive xenograft tumors in mice [30]. Therefore, further clinical characteristics should be considered.

High FASN expression was not found to be related to poor OS in the TCGA-LUSC and TCGA-LUAD cohorts for lung cancer. To avoid incorrect conclusions resulting from FASN expression/clinical information processing, the OncoLnc database was used to perform a Cox regression survival analysis. FASN expression was found to be associated with lung squamous cell carcinoma (Cox coefficient = 0.182, P = 0.0085), but not lung adenocarcinoma. Similar with the results, high FASN expression was associated with poor OS, FP, and PPS in lung adenocarcinoma cases (Supplementary Table 2). Several studies have revealed that FASN can be activated to enhance ERK2 or promote lipogenesis associated with lung adenocarcinoma and it is also expressed in the bronchial epithelium and epithelial hyperplasia in lung squamous cell cancer [31, 32]. Consequently, larger sample sizes or clinical features may be required to confirm the role of FASN in different types of lung cancer.

The analysis of ovarian cancer suggests that a particular regulatory pathway may exist. Although FASN is important for the modulation of cell death in ovarian cancer cells by engaging in a caspase-2 regulatory mechanism [33], high FASN expression was not found to predict poor OS and DFS in ovarian serous cystadenocarcinoma. However, based on the GEO datasets of ovarian cancer, high expression of FASN was found to be related to poor OS in the stage/stage 2/3/4 subgroup, PFS in the histology/serous or TP53/mutated subgroups, and PPS in the histology/serous, debulk/optimal, and chemotherapy/containing platin subgroups (Supplementary Table 3). Consistently, although SIRT3 could enhance invasion and metastasis by improving the expression of FASN in cervical cancer [34], TCGA-based results did not reveal a correlation between high expression of FASN and poor outcome for UCEC.

FASN expression was found to be higher in the STAD group than in the control group. The high expression of FASN has an adverse effect on OS, FP, and PPS in gastric cancer. Accordingly, our results may provide a gene biomarker that could predict OS in patients with gastric cancer. Zhou et al. also reported that FASN is a prognostic marker related to immune infiltration in gastric cancers [35]. Herein, FASN was revealed to have a higher expression in LIHC tissues than the

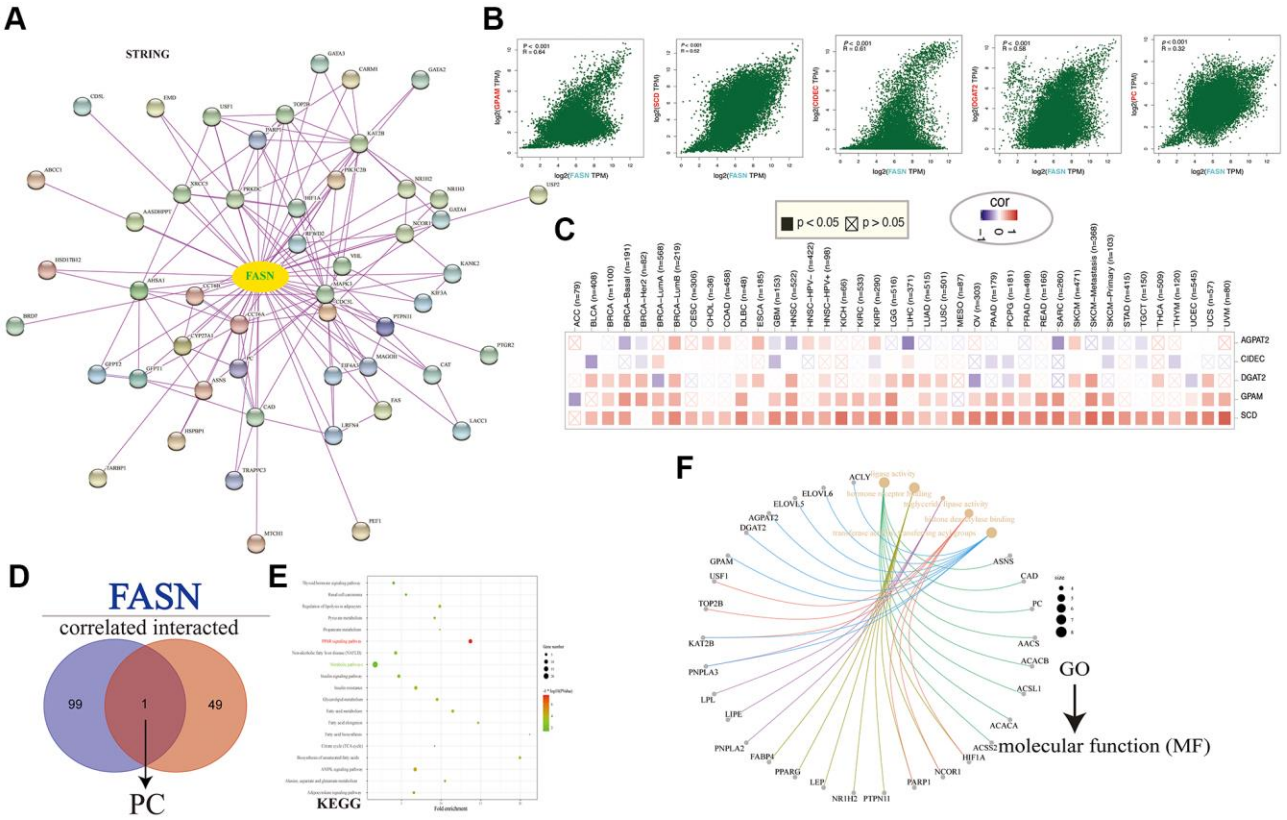

Figure 18. FASN-related gene enrichment analysis. (**A**) FASN-binding proteins. (**B**) Expression correlation between FASN and GPAM, SCD, CIDEC, DGAT2, and PC. (**C**) Corresponding heatmap across cancers. (**D**) The intersection of the FASN-binding and correlated genes. (**E**) KEGG pathway analysis. (**F**) GO (Molecular function) analysis.

corresponding tissues. As hepatocellular carcinoma progression is highly dependent on FASN and its mediated lipogenesis [36], a relationship was found between FASN expression and OS, PFS, RFS, and DSS in liver cancer patients. A meta-analysis further affirmed that FASN may play a cancerous role in various tumors.

In this study, we determined the potential relationship between FASN expression and MSI/TMB across tumors. Prior studies have suggested a negative relationship between FASN expression and TMB or MSI and the clinical outcomes of READ and HNSC [37, 38]. For GBM patients, FASN was found to be highly expressed when the DNA methylation level in the non-promoter region was reduced. Similar findings were obtained for various methylation probes between the GBM group and the normal group of GSE50923. However, the different probes may produce different results. Moreover, glioma patients with isocitrate

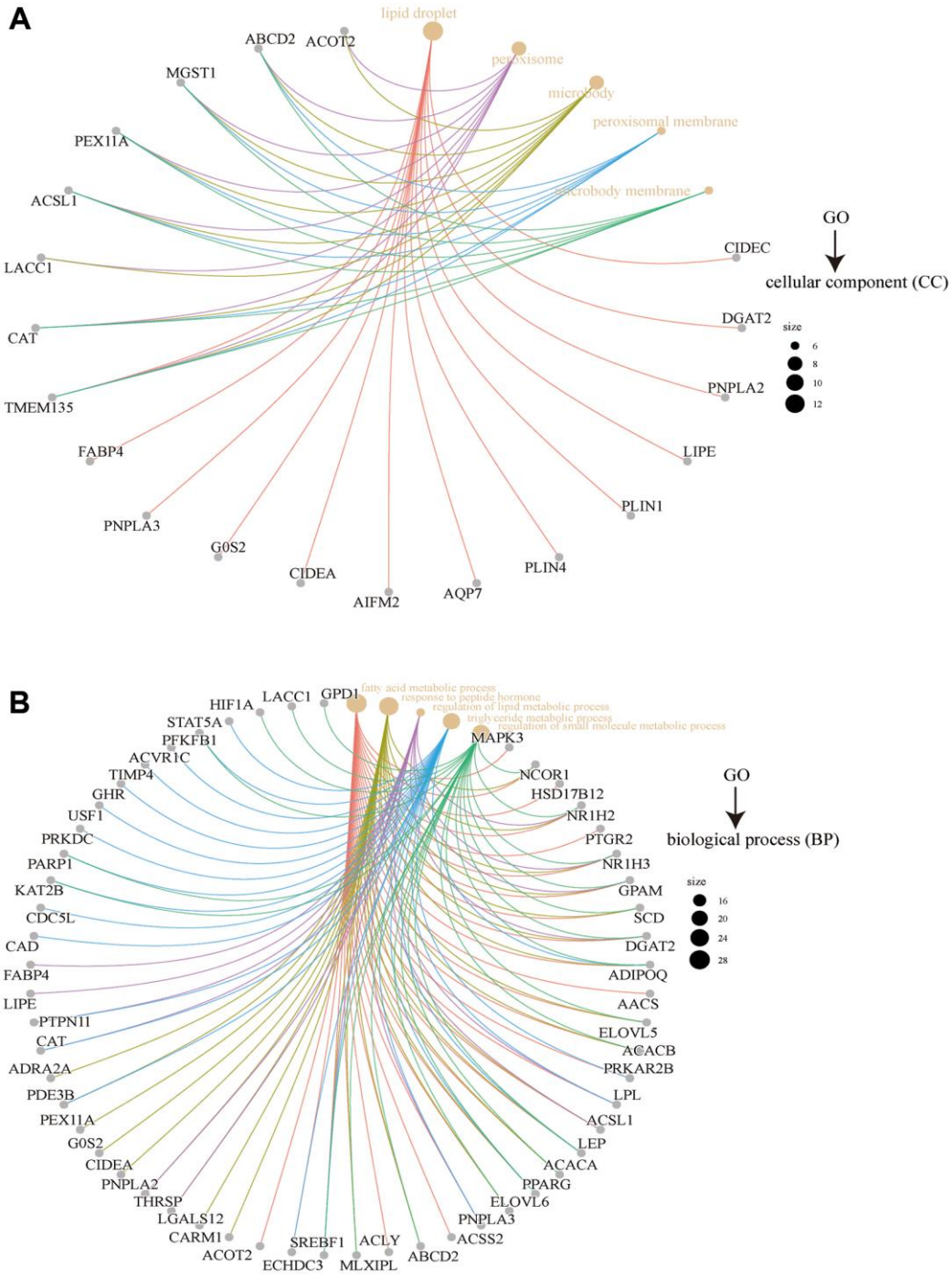

Figure 19. GO analysis of FASN-related genes. Results for cellular component (**A**) and biological process (**B**).

dehydrogenase mutations or wild-type patients had distinct molecular mechanisms (e.g., DNA repair pathways or anti-oxidative pathways) and distinct outcomes [39]. In conclusion, although FASN could enhance the malignant progression of GBM [40], more experiments and clinical trials are needed to verify the results.

The CPTAC dataset was employed to explore the mechanisms of protein and phosphoprotein change in the FASN protein in six types of tumors. Based on the findings, the S207 locus is highly expressed in tumors compared with normal tissues. S207 phosphorylation of FASN has been reported to be essential for molecular responses to pathway activation during biological processes [21, 41]. In addition, lysyl-tRNA synthetase is highly expressed in specific cellular compartments upon phosphorylation in the nucleus after S207 phosphorylation, leading to alternative noncanonical functions in colon cancer [42]. Previously, Motzik et al. found that Ap4A increased the oncogenic activity of melanoma patients and predict a poor outcome, and Ap4A was mainly produced by S207-phosphorylated lysyl-tRNA synthetase [43]. Nevertheless, the specific role of the phosphorylation level of the S207 locus in was not found. More laboratory studies are thus needed to further assess the oncogenic role of FASN phosphorylation and its related regulatory mechanism.

A statistically significant difference was found between FASN and $CD8^+$ T-cells in HNSC, KIRC, OV, and BRCA (Figure 16). These results were consistent with those of published studies, which revealed that phosphatidylinositol 3-kinase α inhibitor could promote fatty acid metabolism to activate CD8+T cells, and a combination of the inhibitor and FASN inhibitor could enhance immunity to decrease breast tumor growth [44]. A favorable relationship was also found between FASN expression and cancer-associated fibroblasts in CESC, KIRC, KIRP, OV, and UVM. Furthermore, a negative correlation was found between FASN expression and CD4+ T cells and NK cells in BLCA, BRCA, and THCA, while a positive correlation was found in HNSC. In conclusion, we hypothesized that FASN plays an oncogenic role through an immune regulatory mechanism.

Based on enrichment analyses carried out using the integrated unit of FASN-binding components and expression-related genes, “hormone receptor binding,” “metabolic pathways,” and “fatty acid metabolic process” may play an important role in the progression of tumors. However, more experiments are needed to assess the oncogenic role of FASN.

Based on a complete analysis across tumors, we found a factual association between FASN expression and clinical outcome, DNA methylation, protein phosphorylation, immune cell infiltration, TMB, or MSI, which could help to better understand the oncogenic role of FASN.

AUTHOR CONTRIBUTIONS

XLH performed the data analysis and assisted with the writing of the manuscript; ZU, MLZ, XLH, KL, LRS, DL, and KW designed the study and assisted with the writing of the manuscript; ZW, XLH, and LW contributed to the writing of the manuscript; YLW, FC, LWZ, and JTZ performed the literature search and collected the data; XLH and LRS analyzed the data. All authors have read and approved the final manuscript.

CONFLICTS OF INTEREST

The authors declare that there are no commercial or financial relationships that could be construed as a potential conflicts of interest.

FUNDING

This work was supported by the National Natural Science Foundation of China (Grant No. 62027813 and 81802683), the Natural Science Foundation of Beijing (Grant No. J180005 and No. 7192056).

REFERENCES

1. Blum A, Wang P, Zenklusen JC. SnapShot: TCGA-Analyzed Tumors. Cell. 2018; 173:530. https://doi.org/10.1016/j.cell.2018.03.059 PMID:29625059

2. Tomczak K, Czerwińska P, Wiznerowicz M. The Cancer Genome Atlas (TCGA): an immeasurable source of knowledge. Contemp Oncol (Pozn). 2015; 19:A68–77. https://doi.org/10.5114/wo.2014.47136 PMID:25691825

3. Clough E, Barrett T. The Gene Expression Omnibus Database. Methods Mol Biol. 2016; 1418:93–110. https://doi.org/10.1007/978-1-4939-3578-9_5 PMID:27008011

4. Asturias FJ, Chadick JZ, Cheung IK, Stark H, Witkowski A, Joshi AK, Smith S. Structure and molecular organization of mammalian fatty acid synthase. Nat Struct Mol Biol. 2005; 12:225–32. https://doi.org/10.1038/nsmb899 PMID:15711565

5. Maier T, Jenni S, Ban N. Architecture of mammalian fatty acid synthase at 4.5 A resolution. Science. 2006; 311:1258–62. https://doi.org/10.1126/science.1123248 PMID:16513975

6. Yu Y, Qiu J, Cao J, Guo Y, Bai H, Wei S, Yan P. Effects of prolonged photoperiod on growth performance, serum lipids and meat quality of Jinjiang cattle in winter. Anim Biosci. 2021; 34:1569–78. https://doi.org/10.5713/ab.20.0750 PMID:33677914

7. Guan X, Okazaki Y, Zhang R, Saito K, Nikolau BJ. Dual-Localized Enzymatic Components Constitute the Fatty Acid Synthase Systems in Mitochondria and Plastids. Plant Physiol. 2020; 183:517–29. https://doi.org/10.1104/pp.19.01564 PMID:32245791

8. Wahlang B, Alexander NC 2nd, Li X, Rouchka EC, Kirpich IA, Cave MC. Polychlorinated biphenyls altered gut microbiome in CAR and PXR knockout mice exhibiting toxicant-associated steatohepatitis. Toxicol Rep. 2021; 8:536–47. https://doi.org/10.1016/j.toxrep.2021.03.010 PMID:33777700

9. Cohen ED, Yee M, Porter GA Jr, Ritzer E, McDavid AN, Brookes PS, Pryhuber GS, O'Reilly MA. Neonatal hyperoxia inhibits proliferation and survival of atrial cardiomyocytes by suppressing fatty acid synthesis. JCI Insight. 2021; 6:e140785. https://doi.org/10.1172/jci.insight.140785 PMID:33507880

10. Deng J, Peng M, Zhou S, Xiao D, Hu X, Xu S, Wu J, Yang X. Metformin targets Clusterin to control lipogenesis and inhibit the growth of bladder cancer cells through SREBP-1c/FASN axis. Signal Transduct Target Ther. 2021; 6:98. https://doi.org/10.1038/s41392-021-00493-8 PMID:33649289

11. Song LR, Li D, Weng JC, Li CB, Wang L, Wu Z, Zhang JT. MicroRNA-195 Functions as a Tumor Suppressor by Directly Targeting Fatty Acid Synthase in Malignant Meningioma. World Neurosurg. 2020; 136:e355–64. https://doi.org/10.1016/j.wneu.2019.12.182 PMID:31927122

12. Menendez JA, Peirce SK, Papadimitropoulou A, Cuyàs E, Steen TV, Verdura S, Vellon L, Chen WY, Lupu R. Progesterone receptor isoform-dependent cross-talk between prolactin and fatty acid synthase in breast cancer. Aging (Albany NY). 2020; 12:24671–92. https://doi.org/10.18632/aging.202289 PMID:33335078

13. Khan A, Aljarbou AN, Aldebasi YH, Allemailem KS, Alsahli MA, Khan S, Alruwetei AM, Khan MA. Fatty Acid Synthase (FASN) siRNA-Encapsulated-Her-2 Targeted Fab'-Immunoliposomes for Gene Silencing in Breast Cancer Cells. Int J Nanomedicine. 2020; 15:5575–89. https://doi.org/10.2147/IJN.S256022 PMID:32801705

14. Kent WJ, Sugnet CW, Furey TS, Roskin KM, Pringle TH, Zahler AM, Haussler D. The human genome browser at UCSC. Genome Res. 2002; 12:996–1006. https://doi.org/10.1101/gr.229102 PMID:12045153

15. Tang Z, Kang B, Li C, Chen T, Zhang Z. GEPIA2: an enhanced web server for large-scale expression profiling and interactive analysis. Nucleic Acids Res. 2019; 47:W556–60. https://doi.org/10.1093/nar/gkz430 PMID:31114875

16. Chen F, Chandrashekar DS, Varambally S, Creighton CJ. Pan-cancer molecular subtypes revealed by mass-spectrometry-based proteomic characterization of more than 500 human cancers. Nat Commun. 2019; 10:5679. https://doi.org/10.1038/s41467-019-13528-0 PMID:31831737

17. Gao J, Aksoy BA, Dogrusoz U, Dresdner G, Gross B, Sumer SO, Sun Y, Jacobsen A, Sinha R, Larsson E, Cerami E, Sander C, Schultz N. Integrative analysis of complex cancer genomics and clinical profiles using the cBioPortal. Sci Signal. 2013; 6:pl1. https://doi.org/10.1126/scisignal.2004088 PMID:23550210

18. Cerami E, Gao J, Dogrusoz U, Gross BE, Sumer SO, Aksoy BA, Jacobsen A, Byrne CJ, Heuer ML, Larsson E, Antipin Y, Reva B, Goldberg AP, et al. The cBio cancer genomics portal: an open platform for exploring multidimensional cancer genomics data. Cancer Discov. 2012; 2:401–404. https://doi.org/10.1158/2159-8290.CD-12-0095 PMID:22588877

19. Lai RK, Chen Y, Guan X, Nousome D, Sharma C, Canoll P, Bruce J, Sloan AE, Cortes E, Vonsattel JP, Su T, Delgado-Cruzata L, Gurvich I, et al. Genome-wide methylation analyses in glioblastoma multiforme. PLoS One. 2014; 9:e89376. https://doi.org/10.1371/journal.pone.0089376 PMID:24586730

20. Stuart SA, Houel S, Lee T, Wang N, Old WM, Ahn NG. A Phosphoproteomic Comparison of B-RAFV600E and MKK1/2 Inhibitors in Melanoma Cells. Mol Cell Proteomics. 2015; 14:1599–615. https://doi.org/10.1074/mcp.M114.047233 PMID:25850435

21. Mertins P, Yang F, Liu T, Mani DR, Petyuk VA, Gillette MA, Clauser KR, Qiao JW, Gritsenko MA, Moore RJ, Levine DA, Townsend R, Erdmann-Gilmore P, et al. Ischemia in tumors induces early and sustained phosphorylation changes in stress kinase pathways but does not affect global protein levels. Mol Cell Proteomics. 2014; 13:1690–704. https://doi.org/10.1074/mcp.M113.036392 PMID:24719451

22. Steven A, Seliger B. The Role of Immune Escape and Immune Cell Infiltration in Breast Cancer. Breast Care (Basel). 2018; 13:16–21. https://doi.org/10.1159/000486585 PMID:29950962

23. Fridman WH, Galon J, Dieu-Nosjean MC, Cremer I, Fisson S, Damotte D, Pagès F, Tartour E, Sautès-Fridman C. Immune infiltration in human cancer: prognostic significance and disease control. Curr Top Microbiol Immunol. 2011; 344:1–24. https://doi.org/10.1007/82_2010_46 PMID:20512556

24. Lim SA, Wei J, Nguyen TM, Shi H, Su W, Palacios G, Dhungana Y, Chapman NM, Long L, Saravia J, Vogel P, Chi H. Lipid signalling enforces functional specialization of T_{reg} cells in tumours. Nature. 2021; 591:306–11. https://doi.org/10.1038/s41586-021-03235-6 PMID:33627871

25. Hu Y, He W, Huang Y, Xiang H, Guo J, Che Y, Cheng X, Hu F, Hu M, Ma T, Yu J, Tian H, Tian S, et al. Fatty Acid Synthase-Suppressor Screening Identifies Sorting Nexin 8 as a Therapeutic Target for NAFLD. Hepatology. 2021; 74:2508–25. https://doi.org/10.1002/hep.32045 PMID:34231239

26. Huang H, Wei Y, Wang J, Ran F, Chen Q. [Effect of fatty acid synthase gene silencing on lipid metabolism and biological behaviors of human hepatoblastoma HepG2 cells]. Nan Fang Yi Ke Da Xue Xue Bao. 2021; 41:747–53. https://doi.org/10.12122/j.issn.1673-4254.2021.05.16 PMID:34134963

27. Breast Cancer Brain Metastases Rely on FASN-Mediated Lipid Biosynthesis. Cancer Discov. 2021; 11:1315. https://doi.org/10.1158/2159-8290.CD-RW2021-051 PMID:33837062

28. Giró-Perafita A, Palomeras S, Lum DH, Blancafort A, Viñas G, Oliveras G, Pérez-Bueno F, Sarrats A, Welm AL, Puig T. Preclinical Evaluation of Fatty Acid Synthase and EGFR Inhibition in Triple-Negative Breast Cancer. Clin Cancer Res. 2016; 22:4687–97. https://doi.org/10.1158/1078-0432.CCR-15-3133 PMID:27106068

29. Menendez JA, Lupu R. Fatty acid synthase regulates estrogen receptor-α signaling in breast cancer cells. Oncogenesis. 2017; 6:e299. https://doi.org/10.1038/oncsis.2017.4 PMID:28240737

30. Menendez JA, Papadimitropoulou A, Vander Steen T, Cuyàs E, Oza-Gajera BP, Verdura S, Espinoza I, Vellon L, Mehmi I, Lupu R. Fatty Acid Synthase Confers Tamoxifen Resistance to ER+/HER2+ Breast Cancer. Cancers (Basel). 2021; 13:1132. https://doi.org/10.3390/cancers13051132 PMID:33800852

31. Piyathilake CJ, Frost AR, Manne U, Bell WC, Weiss H, Heimburger DC, Grizzle WE. The expression of fatty acid synthase (FASE) is an early event in the development and progression of squamous cell carcinoma of the lung. Hum Pathol. 2000; 31:1068–73. https://doi.org/10.1053/hupa.2000.9842 PMID:11014573

32. Gouw AM, Eberlin LS, Margulis K, Sullivan DK, Toal GG, Tong L, Zare RN, Felsher DW. Oncogene KRAS activates fatty acid synthase, resulting in specific ERK and lipid signatures associated with lung adenocarcinoma. Proc Natl Acad Sci U S A. 2017; 114:4300–305. https://doi.org/10.1073/pnas.1617709114 PMID:28400509

33. Yang CS, Matsuura K, Huang NJ, Robeson AC, Huang B, Zhang L, Kornbluth S. Fatty acid synthase inhibition engages a novel caspase-2 regulatory mechanism to induce ovarian cancer cell death. Oncogene. 2015; 34:3264–72. https://doi.org/10.1038/onc.2014.271 PMID:25151963

34. Xu LX, Hao LJ, Ma JQ, Liu JK, Hasim A. SIRT3 promotes the invasion and metastasis of cervical cancer cells by regulating fatty acid synthase. Mol Cell Biochem. 2020; 464:11–20. https://doi.org/10.1007/s11010-019-03644-2 PMID:31677030

35. Zhou Y, Su W, Liu H, Chen T, Höti N, Pei H, Zhu H. Fatty acid synthase is a prognostic marker and associated with immune infiltrating in gastric cancers precision medicine. Biomark Med. 2020; 14:185–99. https://doi.org/10.2217/bmm-2019-0476 PMID:31904263

36. Li L, Che L, Tharp KM, Park HM, Pilo MG, Cao D, Cigliano A, Latte G, Xu Z, Ribback S, Dombrowski F, Evert M, Gores GJ, et al. Differential requirement for de novo lipogenesis in cholangiocarcinoma and

hepatocellular carcinoma of mice and humans. Hepatology. 2016; 63:1900–13. https://doi.org/10.1002/hep.28508 PMID:26910791

37. Chen EX, Jonker DJ, Loree JM, Kennecke HF, Berry SR, Couture F, Ahmad CE, Goffin JR, Kavan P, Harb M, Colwell B, Samimi S, Samson B, et al. Effect of Combined Immune Checkpoint Inhibition vs Best Supportive Care Alone in Patients With Advanced Colorectal Cancer: The Canadian Cancer Trials Group CO.26 Study. JAMA Oncol. 2020; 6:831–38. https://doi.org/10.1001/jamaoncol.2020.0910 PMID:32379280

38. Demokan S, Suoglu Y, Demir D, Gozeler M, Dalay N. Microsatellite instability and methylation of the DNA mismatch repair genes in head and neck cancer. Ann Oncol. 2006; 17:995–99. https://doi.org/10.1093/annonc/mdl048 PMID:16569647

39. Liu Y, Lang F, Chou FJ, Zaghloul KA, Yang C. Isocitrate Dehydrogenase Mutations in Glioma: Genetics, Biochemistry, and Clinical Indications. Biomedicines. 2020; 8:294. https://doi.org/10.3390/biomedicines8090294 PMID:32825279

40. Lee JE, Lim JH, Hong YK, Yang SH. High-Dose Metformin Plus Temozolomide Shows Increased Anti-tumor Effects in Glioblastoma In Vitro and In Vivo Compared with Monotherapy. Cancer Res Treat. 2018; 50:1331–42. https://doi.org/10.4143/crt.2017.466 PMID:29334602

41. Van Hoof D, Muñoz J, Braam SR, Pinkse MW, Linding R, Heck AJ, Mummery CL, Krijgsveld J. Phosphorylation dynamics during early differentiation of human embryonic stem cells. Cell Stem Cell. 2009; 5:214–26. https://doi.org/10.1016/j.stem.2009.05.021 PMID:19664995

42. Nam SH, Kim D, Lee D, Lee HM, Song DG, Jung JW, Kim JE, Kim HJ, Kwon NH, Jo EK, Kim S, Lee JW. Lysyl-tRNA synthetase-expressing colon spheroids induce M2 macrophage polarization to promote metastasis. J Clin Invest. 2018; 128:5034–55. https://doi.org/10.1172/JCI99806 PMID:30188867

43. Motzik A, Amir E, Erlich T, Wang J, Kim BG, Han JM, Kim JH, Nechushtan H, Guo M, Razin E, Tshori S. Post-translational modification of HINT1 mediates activation of MITF transcriptional activity in human melanoma cells. Oncogene. 2017; 36:4732–38. https://doi.org/10.1038/onc.2017.81 PMID:28394346

44. Sun P, Zhang X, Wang RJ, Ma QY, Xu L, Wang Y, Liao HP, Wang HL, Hu LD, Kong X, Ding J, Meng LH. PI3Kα inhibitor CYH33 triggers antitumor immunity in murine breast cancer by activating $CD8^+$T cells and promoting fatty acid metabolism. J Immunother Cancer. 2021; 9:e003093. https://doi.org/10.1136/jitc-2021-003093 PMID:34373258

SUPPLEMENTARY MATERIALS

Supplementary Figures

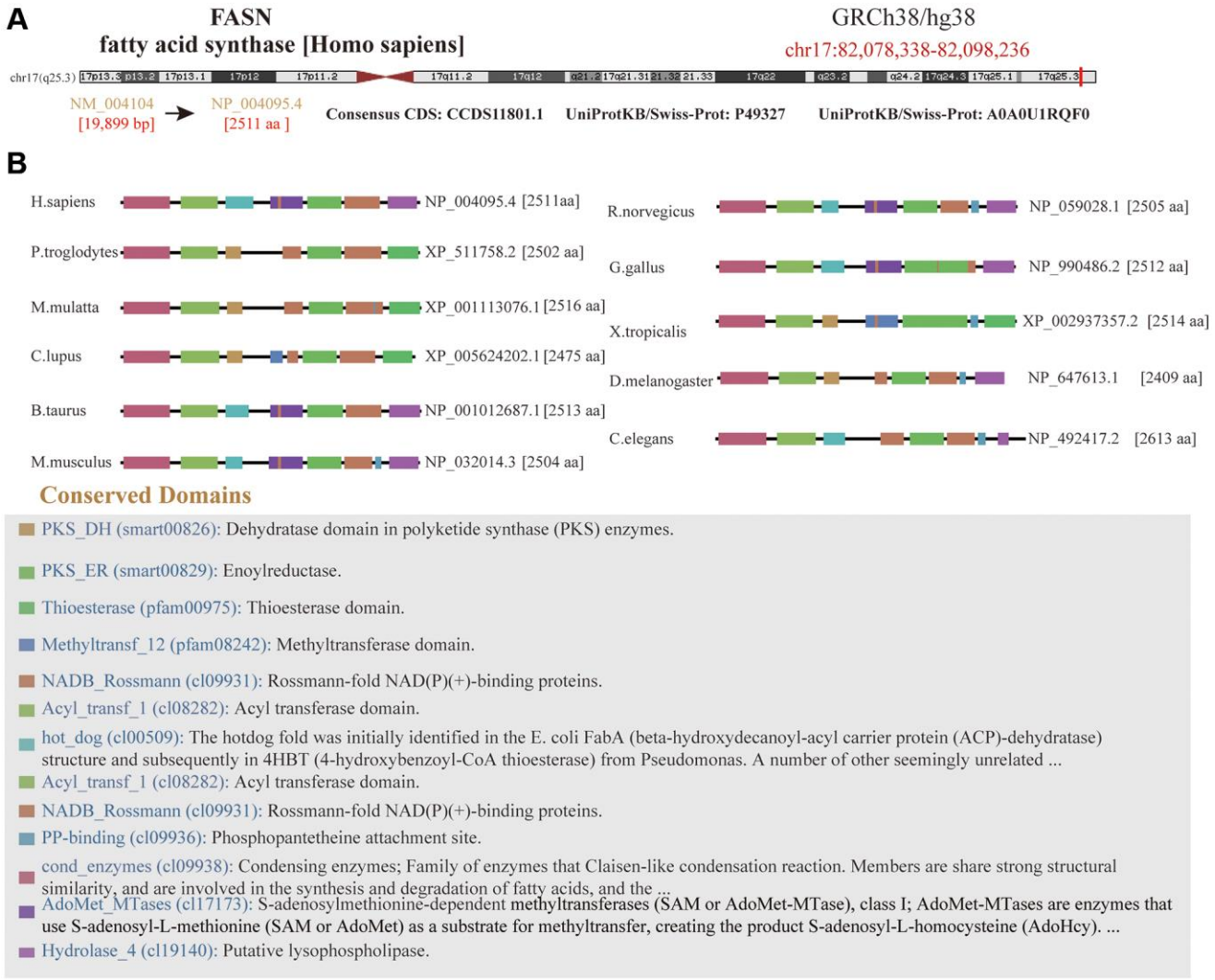

Supplementary Figure 1. Structural characteristics of FASN across various species. (**A**) Genomic location of FASN; (**B**) Conserved domains of the FASN protein.

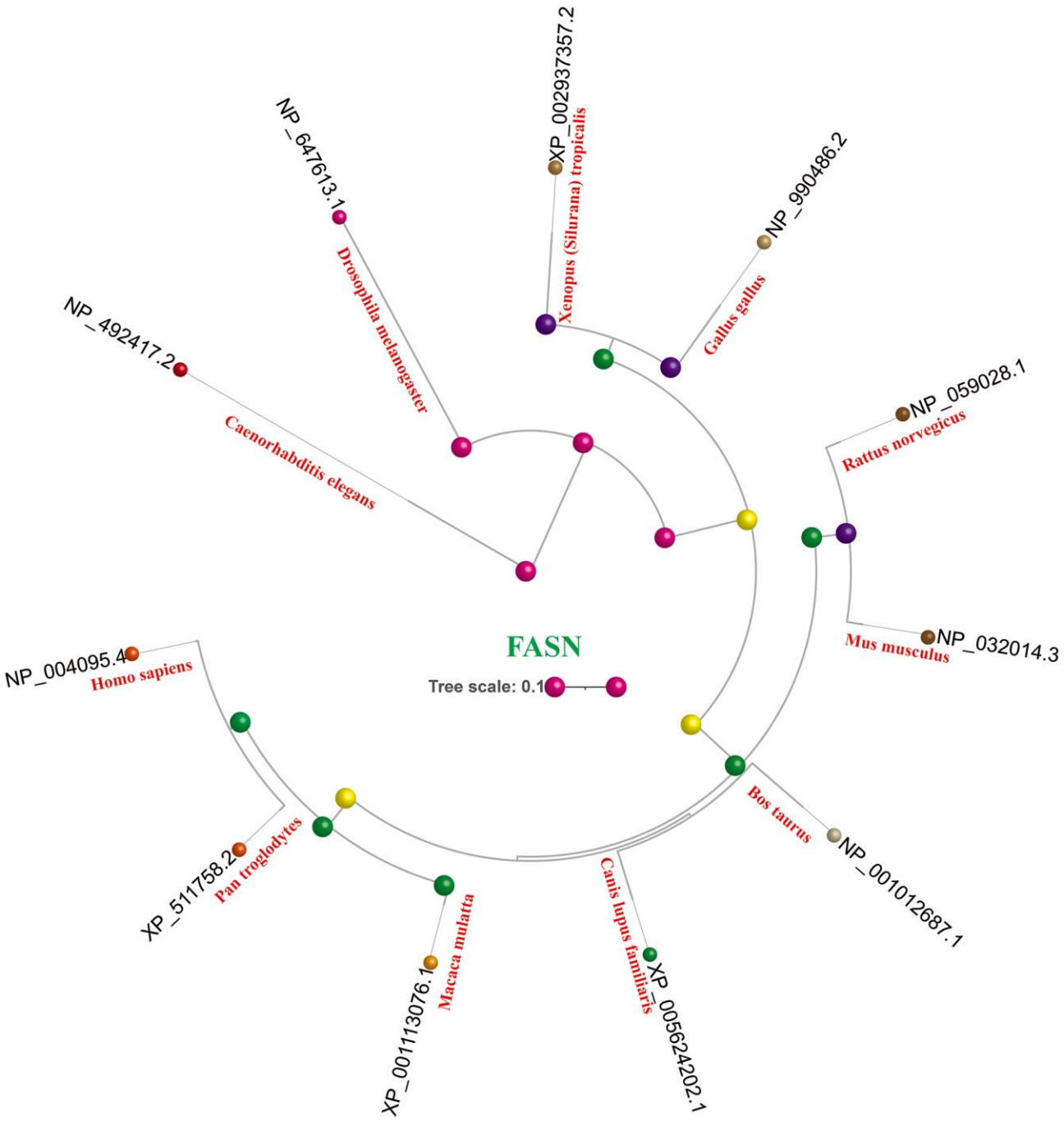

Supplementary Figure 2. Phylogenetic tree of FASN.

Supplementary Tables

Please browse Full Text version to see the data of Supplementary Table 7.

Supplementary Table 1. Correlation of FASN and the outcome of breast cancer in subgroup analysis.

Factor	Subgroup	Sample size	OS		RFS		DMFS		PPS	
			HR	*P*	HR	*P*	HR	*P*	HR	*P*
ER status	ER positive	3499	1.22	0.2314	0.89	0.1831	1.14	0.3469	1.14	0.3469
	ER negative	2168	0.61	**0.0279**	0.84	0.0802	0.72	**0.0403**	0.72	**0.0403**
TP53 status	mutated	272	0.68	0.2892	1.55	0.075	0.56	0.2083	0.56	0.2083
	Wild type	388	1.6	0.2105	2.11	**0.0058**	2.65	**0.0192**	2.65	**0.0192**
PR status	PR positive	1559	2.27	0.0673	0.84	0.3087	0.81	**0.3891**	0.81	**0.3891**
	PR negative	1989	1.39	0.1936	0.81	0.0793	1.4	0.0621	1.4	0.0621
HER2 status	HER2 positive	1273	0.67	**0.0299**	0.78	0.053	0.77	0.1802	0.77	0.1802
	HER2 negative	6262	0.73	**0.0058**	0.71	**7.1e-09**	0.63	**2.9e-07**	0.63	**2.9e-07**
Grade	Grade 1	576	0.38	**0.0394**	0.39	**0.0103**	0.57	0.1728	0.57	0.1728
	Grade 2	1795	1.57	0.0543	1.14	0.3026	0.77	0.0714	0.77	0.0714
	Grade 3	2058	0.74	0.0549	0.83	0.0503	0.71	**0.0096**	0.71	**0.0096**
Intrinsic subtype	Basal	1494	0.81	0.2772	0.57	**4.7e-07**	0.78	0.1367	0.78	0.1367
	Luminal A	3511	0.77	0.1388	0.79	**0.0108**	0.82	0.1539	0.82	0.1539
	Luminal B	2015	0.82	0.3014	0.75	**0.0091**	0.69	**0.0094**	0.69	**0.0094**
	HER2+	515	0.37	**0.0005**	0.7	**0.0497**	0.64	0.0777	0.64	0.0777
Lymph node status	Lymph node positive	2153	0.61	**0.0037**	0.69	**1.1e-05**	0.55	**2.5e-06**	0.55	**2.5e-06**
	Lymph node negative	2829	0.69	0.0596	0.85	0.0779	0.65	**0.0016**	0.65	**0.0016**
Pietenpol subtype	Basal-like 1	418	1.65	0.2114	0.52	**0.0047**	1.69	0.096	1.69	0.096
	Basal-like 2	165	5.76	**0.0002**	1.64	0.1821	1.93	0.0823	1.93	0.0823
	immunomodulatory	462	0.54	0.1878	0.6	0.0434	0.46	**0.0304**	0.46	**0.0304**
	Mesenchymal	382	0.39	**0.0084**	0.46	**0.0001**	0.51	**0.0281**	0.51	**0.0281**
	Mesenchymal stem-like	201	0.27	**0.0074**	0.41	**0.0125**	0.37	0.0502	0.37	0.0502
	Luminal androgen receptor	413	0.4	**0.002**	0.56	**0.0033**	0.66	**0.1525**	0.66	**0.1525**

Abbreviations: HR: hazard ratio; OS: overall survival; RFS: relapse free survival; DMFS: distant metastasis free survival; ER: Estrogen receptor; PR: Progesterone receptor; HER2: human epidermal growth factor receptor-2; TP53: Tumor Protein P53; NA: not available data. *P* value less than 0.05 is shown in bold.

Supplementary Table 2. Correlation of FASN and the outcome of lung cancer in subgroup analysis.

Factor	Subgroup	Sample size	OS		FP		PPS	
			HR	*P*	HR	*p*	*HR*	*p*
Histology	adenocarcinoma	865	2.14	**9.4e-09**	1.49	**0.0129**	1.84	**0.0097**
	squamous cell carcinoma	675	1.2	0.1415	1.38	0.2151	0.35	0.0645
gender	female	817	2.54	**5.8e-09**	2.01	**7.8e-05**	1.77	**0.0064**
	male	1387	1.29	**0.0013**	1.7	**7.2e-05**	1.45	**0.0463**
smoking history	exclude those never smoked	970	1.74	**3.0e-05**	1.55	**0.0004**	1.16	0.3048
	only those never smoked	247	3.44	**2.3e-05**	2.05	**0.0026**	2.6	**0.0031**
stage	stage I	652	3.16	**0.0157**	0.34	**0.0046**	3.22	**0.0358**
	stage II	320	2.47	0.1393	3.46	**0.009**	NA	NA
grade	grade II	310	2.52	**0.0107**	0.23	0.0613	NA	NA
AJCC stage t	t1	475	1.26	0.1213	3.12	0.0841	NA	NA
	t2	686	0.52	0.1526	0.67	0.3663	0.69	**0.5304**
AJCC stage n	n0	863	0.39	**0.0396**	1.99	0.1257	1.89	0.4025
AJCC stage m	m0	818	0.46	0.1932	0.23	**0.0117**	NA	NA
surgery	only surgical margins negative	730	3.84	**0.0001**	2.93	**9.4e-05**	2.78	**0.0078**
radiotherapy	no	276	0.39	0.1143	0.48	0.2646	NA	NA
chemotherapy	no	317	1.52	0.4613	2.26	0.2962	NA	NA

Abbreviations: HR: hazard ratio; AJCC: American Joint Committee on Cancer; OS: overall survival; FP: first progression; PPS: post progression survival; NA: not available data. *P* value less than 0.05 is shown in bold.

Supplementary Table 3. Correlation of FASN and the outcome of ovarian cancer in subgroup analysis.

Factor	Subgroup	Sample size	OS		PFS		PPS	
			HR	*p*	HR	*p*	HR	*p*
Histology	Endometrioid	62	3.28	0.1677	3.89	0.1548	NA	NA
	Serous	1232	1.13	0.1439	1.29	**0.0014**	1.31	**0.0043**
Stage	Stage 1	107	1.89	0.2613	2.28	0.1184	NA	NA
	Stage 2	72	1.88	**0.2354**	3.01	**0.0326**	2.69	0.0923
	Stage 3	1079	0.88	**0.122**	1.22	**0.0161**	1.22	**0.048**
	Stage 4	189	1.57	**0.018**	1.33	0.1413	1.39	0.1421
Grade	Grade 1	56	1.52	0.3954	0.44	0.1315	NA	NA
	Grade 2	325	0.78	0.1418	1.4	0.0592	1.33	0.1478
	Grade 3	1024	0.87	0.0895	1.17	0.0627	1.23	**0.0597**
	Grade 4	21	0.59	0.3614	NA	NA	NA	NA
TP53 mutation	Mutated	516	1.4	**0.0036**	1.57	**0.0001**	1.53	**0.0008**
	Wild type	102	1.84	**0.0272**	0.71	0.2007	2.05	**0.0193**
Debulk	optimal	802	0.64	**1.5e-05**	0.74	**0.0023**	0.7	**0.0064**
	suboptimal	536	0.83	0.1182	0.85	0.1764	1.43	**0.0077**
Chemotherapy	Contains platin	1438	0.92	**0.2755**	0.86	**0.0343**	1.28	**0.0056**
	Contains Taxol	821	0.78	**0.0105**	0.79	**0.0108**	1.17	0.1722
	Contains Taxol+platin	804	0.8	**0.021**	0.82	**0.0314**	1.17	0.1647
	Contains Avastin	50	0.64	0.3165	1.54	0.2075	0.62	0.286
	Contains Docetaxel	108	1.47	0.233	1.53	0.0853	1.57	0.2054
	Contains Gemcitabine	135	0.73	0.1477	0.73	0.1155	0.67	0.0739
	Contains Paclitaxel	248	1.5	0.0856	1.58	**0.0076**	1.68	0.0506
	Contains Topotecan	119	0.56	**0.0097**	1.26	0.2572	0.56	**0.0068**

Abbreviations: HR: hazard ratio; OS: overall survival; PFS: progress free survival; PPS: post progression survival; TP53: Tumor Protein P53; NA: not available data. *P* value less than 0.05 is shown in bold.

Supplementary Table 4. Correlation of FASN and outcome of gastric cancer in subgroup analysis.

Factor	Subgroup	Sample size	OS		FP		PPS	
			HR	*P*	HR	*P*	HR	*P*
Gender	Female	244	2.2	**1.0e-05**	2.06	**0.0001**	2.67	**2.3e-06**
	Male	566	2.34	**2.1e-12**	2.18	**9.8e-11**	3.25	**< 1e-16**
Stage	Stage 1	69	3.41	**0.0263**	2.33	**0.1551**	4.08	**0.0474**
	Stage 2	145	1.85	0.0506	1.63	0.1271	1.83	0.067
	Stage 3	319	2.26	**1.3e-06**	1.94	**0.0008**	2.75	**2.6e-06**
	Stage 4	152	1.57	**0.023**	1.54	**0.0349**	1.82	**0.0135**
Stage t	t2	253	1.87	**0.0044**	1.78	**0.006**	2.08	**0.0016**
	t3	208	1.76	**0.0014**	1.6	**0.0128**	2.42	**4.8e-06**
	t4	39	0.72	0.4482	1.37	0.4223	0.48	0.1121
Stage n	n0	76	1.81	0.1747	1.76	0.1894	0.55	0.3446
	n1	232	2.13	**0.0002**	2.15	**0.0008**	3.3	**2.3e-07**
	n2	129	2.46	**7.0e-05**	2.01	**0.0014**	2.62	**6.5e-05**
	n3	76	1.54	0.1166	1.44	0.1824	1.56	0.146
Stage m	m0	459	1.72	**0.0001**	1.53	**0.0015**	2.38	**6.9e-09**
	m1	58	1.78	**0.0493**	1.37	0.2871	3.15	**0.0037**
HER2	negative	641	1.92	**1.6e-08**	1.95	**6.9e-07**	2.56	**1.9e-10**
	positive	424	1.89	**3.9e-05**	2.59	**6.6e-09**	5.07	**3.1e-11**
Lauren classification	Intestinal	336	2.53	**5.3e-09**	1.94	**0.0004**	3.87	**2.6e-11**
	Diffuse	248	1.76	**0.0029**	1.61	**0.0115**	1.61	**0.0195**
	Mixed	33	0.36	0.1051	0.44	0.1198	NA	NA
Differentiation	Poorly	166	1.36	0.1344	1.34	0.2102	1.35	0.3727
	Moderately	67	1.64	0.1359	1.42	0.3195	4.23	**0.0032**
	Well	32	2.06	0.1872	NA	NA	NA	NA
Treatment	Surgery alone	393	1.43	**0.0162**	1.25	0.1168	2.24	**1.4e-06**
	5-Fu based adjuvant	157	1.88	**0.001**	1.97	**0.0001**	1.24	0.238
Perforation	No	169	1.15	0.4961	1.2	0.3664	1.74	0.0633

Abbreviations: HR: hazard ratio; OS: overall survival; FP: first progression; PPS: post progression survival; HER2: human epidermal growth factor receptor-2; NA: not available data. *P* value less than 0.05 is shown in bold.

Supplementary Table 5. Correlation of FASN and outcome of liver cancer in subgroup analysis.

Factor	Subgroup	Sample size	OS		PFS		RFS		DSS	
			HR	*P*	HR	*P*	HR	*P*	HR	*P*
Stage	Stage 1	171	1.56	0.2807	0.73	0.2046	0.62	0.0792	0.34	0.0685
	Stage 2	86	2.73	0.0562	2.15	**0.0134**	2.3	**0.0164**	2.35	0.1307
	Stage 3	85	0.53	0.0511	1.54	0.1182	1.71	0.0763	0.58	0.1695
Grade	Grade 1	55	0.56	0.2875	0.63	0.2346	0.33	**0.0199**	0.5	0.3097
	Grade 2	177	2.01	**0.0105**	1.77	**0.0182**	1.8	**0.0205**	2.58	**0.0053**
	Grade 3	122	1.41	0.2612	1.74	**0.0297**	1.64	0.0713	1.43	0.347
AJCC_T	T1	181	1.51	0.2861	0.79	0.3241	0.67	0.1283	0.62	0.3015
	T2	94	1.99	0.0654	2.09	**0.0106**	2.4	**0.0073**	2.03	0.1478
	T3	80	0.39	**0.0036**	1.53	0.1383	1.68	0.0998	0.4	**0.0204**
Gender	Female	121	1.72	0.059	1.48	0.165	1.39	0.3534	1.57	0.3201
	Male	250	0.78	0.2945	1.34	0.1135	1.39	0.1314	1.4	0.2392
Vascular invasion	None	205	0.8	0.4055	1.35	0.2039	1.29	0.3093	0.73	0.3937
	micro	93	1.95	0.1742	0.56	**0.045**	0.58	0.0935	0.32	**0.0487**
Race	White	184	0.65	0.0851	0.7	0.0699	0.69	0.1061	0.69	0.2204
	Asian	158	2.13	0.0605	1.73	**0.0228**	1.83	**0.0183**	2.22	0.133
Sorafenib treatment	treated	30	1.97	0.2196	0.49	0.101	0.57	0.2987	1.97	0.2196
Alcohol consumption	Yes	117	1.98	0.1211	2.03	**0.0386**	1.78	0.0651	2.05	0.0562
	none	205	1.31	0.3425	0.63	**0.0249**	0.6	**0.0245**	0.55	0.0612
Hepatitis virus	Yes	153	0.49	0.0806	1.3	0.2643	1.35	0.2444	0.44	0.1206
	none	169	1.59	**0.0482**	1.41	0.1555	0.78	0.3237	1.69	0.0771

Abbreviations: HR: hazard ratio; AJCC: American Joint Committee on Cancer; OS: overall survival; PFS: progress free survival; RFS: relapse free survival; DSS: disease specific survival; NA: not available data. *P* value less than 0.05 is shown in bold.

Supplementary Table 6. Phosphorylation locus of FASN.

site	sequence	experimentally confirmed[#]	hydrophobicity	*p*-site similarity score	maximum kinase specificity	sum kinase specificity score	conservation score
S207	FLRLGMLSPEGTCKA	24719451; 25850435	0.253	–57.6	516	20,583	42.7
S724	IPEAQWHSSLARTSS	20068231	–0.827	–59.2	273	12,141	30.9
S725	PEAQWHSLARTSSA	20068231	–1.007	–57.5	353	15,253	16.4
T976	FDHPESPTPNPTEPL	18669648	–1.440	–54.8	278	9,657	9.7
S1174	AQIPRDPSQQELPRL	27251275	–1.267	–55.3	572	20,371	4.6
S1411	RRPTPQDSPIFLPVD	18669648	–0.860	–56.2	549	21,758	10.6
S2198	SSKADEASELACPTP	18669648	–0.760	–55.9	289	13,190	1.5
T2204	ASELACPTPKEDGLA	15302935	–0.320	–55.5	283	9,599	14.2

[#]The PMID (PubMed Unique Identifier) information of the publication was provided.

Supplementary Table 7. Correlation of FASN with FASN CD4+ T-cells and NK cells based on the TIMER2 database.